HHS Public Access

Author manuscript

Glia. Author manuscript; available in PMC 2021 July 01.

Published in final edited form as:

Glia. 2020 July ; 68(7): 1445–1465. doi:10.1002/glia.23792.

Inflammation and matrix metalloproteinase 9 (Mmp-9) regulate photoreceptor regeneration in adult zebrafish

Nicholas J. Silva[1,2], **Mikiko Nagashima**[2], **Jingling Li**[3], **Laura Kakuk-Atkins**[2], **Milad Ashrafzadeh**[2], **David R. Hyde**[3], **Peter F. Hitchcock**[1,2]

[1]Neuroscience Graduate Program, University of Michigan, Ann Arbor, MI 48109

[2]Department of Ophthalmology and Visual Sciences, University of Michigan, Ann Arbor, MI 48105

[3]Department of Biological Sciences, University of Notre Dame, Notre Dame, IN, 46556

Abstract

Brain injury activates complex inflammatory signals in dying neurons, surviving neurons, and glia. Here, we establish that inflammation regulates the regeneration of photoreceptors in the zebrafish retina and determine the cellular expression and function of the inflammatory protease, matrix metalloproteinase 9 (Mmp-9), during this regenerative neurogenesis. Following photoreceptor ablation, anti-inflammatory treatment suppresses the number of injury-induced progenitors and regenerated photoreceptors. Upon photoreceptor injury, *mmp-9* is induced in Müller glia and Müller glia-derived photoreceptor progenitors. Deleting *mmp-9* results in over production of injury-induced progenitors and regenerated photoreceptors, but over time the absence of Mmp-9 compromises the survival of the regenerated cones. At all time-points studied, the levels of *tnf–a* are significantly elevated in mutant retinas. Anti-inflammatory treatment in mutants rescues the defects in cone survival. These data provide a link between injury-induced inflammation in the vertebrate CNS, Mmp-9 function during neuronal regeneration and the requirement of Mmp-9 for the survival of regenerated cones.

Graphical Abstract

Corresponding Author: Peter F. Hitchcock, University of Michigan, Department of Ophthalmology and Visual Sciences, W.K. Kellogg Eye Center, 1000 Wall Street, Ann Arbor, MI 48105, peterh@med.umich.edu, 734-763-8169.

Conflict of Interest Statement:
The authors declare no competing financial interests.

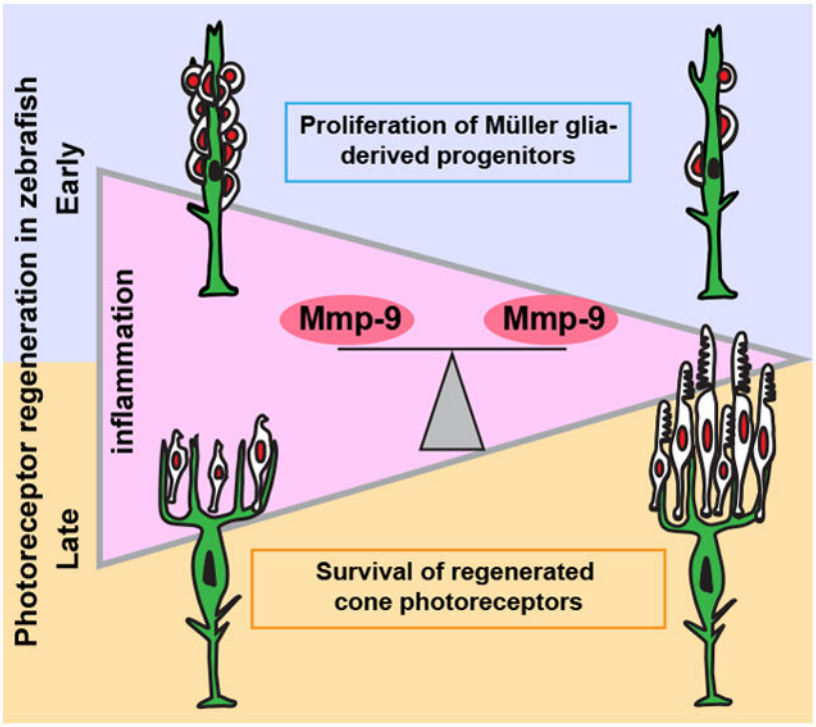

Keywords

Immunosuppression; Müller glia; microglia; cytokines; proliferation; stem cell

Introduction

Inflammation modulates immune and nonimmune functions during tissue development, repair, and disease (Deverman and Patterson, 2009; Ekdahl et al., 2009). Acute inflammation involves the secretion of proinflammatory cytokines and chemokines that recruit immune cells to the damaged tissue (Liddiard et al., 2011; Nathan, 2002). In the central nervous system of adult mammals, acute inflammation can activate signaling cascades in stem and progenitor cells that stimulate proliferation and promote neurogenesis (Borsini et al., 2015; Ekdahl et al., 2009; Kizil et al., 2015; Kyritsis et al., 2014, 2012). Chronic inflammation, however, is detrimental, and results in secondary damage to neurons and, in severe cases, neurodegenerative disease (Amor et al., 2010). Proper regulation of inflammatory cascades in the central nervous system is critical both to maintain tissue homeostasis and repair brain injuries.

Unlike mammals, which possess a limited capacity for tissue regeneration, zebrafish have the ability to regenerate tissues and organs, such as fins, heart, brain, spinal cord, and retina (Gemberling et al., 2013; Kizil et al., 2012; Lenkowski and Raymond, 2014). Studies using zebrafish have identified cellular and molecular mechanisms which may unlock the regenerative potential of mammalian tissues (Ueki et al., 2015; Martin and Poché, 2019). Such mechanisms include inflammation. In zebrafish acute inflammation is both necessary

and sufficient to induce neuronal regeneration (Kyritsis et al., 2012; White et al., 2017; Caldwell et al., 2019).

In the injured zebrafish retina, Müller glia serve as intrinsic stem cells that endow this nervous tissue the ability to regenerate (Bernardos et al., 2007; Fausett and Goldman, 2006). Neuronal injury and death stimulate Müller glia to initiate a transient gliotic response, followed by partial dedifferentiation and entry into the cell cycle (Raymond et al., 2006; Thomas et al., 2016). Müller glia then undergo a single asymmetric division to produce multipotent progenitors, which proliferate rapidly, migrate to areas of cell death and differentiate to replace the ablated neurons (Fimbel et al., 2007; Sherpa et al., 2008; Nagashima et al., 2013; Goldman, 2014; Gorsuch and Hyde, 2014; Lenkowski and Raymond, 2014). In the zebrafish retina, paracrine and autocrine signaling play essential roles in facilitating this regenerative neurogenesis (Nelson et al., 2013; Zhao et al., 2014). Dying photoreceptors secrete Tnf-α, to which Müller glia respond by reprogramming into a stem cell-state, synthesizing Tnf−α and entering into the cell cycle (Nelson et al., 2013). Also, *leptin* and Il-6 family cytokines expressed by Müller glia and Müller glia-derived progenitors are required for injury-induced proliferation (Zhao et al., 2014).

Based on their structure and specific substrates, matrix metalloproteinases (Mmps) are classified into five groups: gelatinases, collagenases, MTMMPs, stromelysins, and matrilysins (Vandooren, et al., 2013b). Matrix metalloproteinase 9 (Mmp-9) is a secreted gelatinase, first purified from neutrophils and monocytes stimulated by IL-8 and IL-1β (Masure et al. 1991; Opdenakker, et al., 1991). During tissue development and homeostasis, Mmp-9 plays a prominent role by acting on extracellular molecules, including adhesion molecules, growth factors and cytokines (Bonnans et al., 2014; Le et al., 2007; Masure et al., 1991; Parks et al., 2004; Vandooren et al., 2013b, 2014), which can regulate proliferation, cellular migration and cellular differentiation. It is well established that inflammatory cytokines can induce the expression of Mmp-9 (Vecil et al., 2000; Shubayev et al., 2006; Nagase, et al., 2006; Vandooren, et al., 2013b). In turn, Mmp-9 can cleave cytokine precursors and mature cytokines into activate and inactivate forms, respectively, revealing the complex role of Mmp-9 in modulating inflammation (Parks et al., 2004). The complexities of Mmp-9 function suggest its role during regeneration is likely tissue, substrate and injury-context dependent (Hindi et al., 2013; Vandooren et al., 2014; Ando et al., 2017; Xue et al., 2017). The cellular expression and function of Mmp-9 during photoreceptor regeneration in the zebrafish are unknown.

Here, we use zebrafish to determine the general role of inflammation and the cellular expression and function of the matrix metalloproteinase, Mmp-9, during photoreceptor regeneration. We establish that in the adult retina inflammation governs the proliferation of Müller glia-derived progenitors. We show that *mmp-9* is expressed in Müller glia, as they prepare to enter the cell cycle, and Müller glia-derived progenitors. Using loss-of-function mutants, we determine that Mmp-9 negatively regulates the proliferation of Müller glia-derived progenitors. In mutants both unlesioned and lesioned retinas show elevated expression of the inflammatory cytokine, *tnf−α*. Finally, we demonstrate that following photoreceptor regeneration, Mmp-9 is required for the survival of regenerated cone photoreceptors.

Materials and Methods

Animals

Wild-type, AB strain zebrafish (*Danio rerio*; ZIRC, University of Oregon, Eugene, OR) were propagated, maintained, and housed in recirculating habitats at 28.5°C and on a 14/10-h light/dark cycle. Embryos were collected after natural spawns, incubated at 28.5°C and staged by hours post fertilization (hpf). Adults were of either sex and used between 6 and15 months of age. Ages of animals were matched within experiments. The transgenic reporter lines, *Tg[gfap:EGFP]*^{mi2002} and *Tg[mpeg1:mCherry]*^{gl23} were used to identify Müller glia and microglia, respectively (Bernardos and Raymond, 2006; Ellett et al., 2011). All experimental protocols were approved by the University of Michigan's Institutional Animal Care and Use Committee (IACUC).

Light Lesions

To kill photoreceptors, fish were dark adapted, then exposed to high intensity light (ca. 100,000 lux) for 30 minutes, followed by exposure to constant light (ca. 30.000 lux) for 72 hours (Taylor et al., 2015). After 72 hours fish were returned to the recirculating habitats and normal light/dark cycle.

Quantitative Real-Time PCR

Total RNA was extracted from dissected whole retinas using TRIzol (Invitrogen, Carlsbad, CA). Reverse transcription to cDNA was performed using 1 μg RNA (Qiagen QuantiTect Reverse Transcription kit; Venlo, Netherlands), and each qPCR reaction was performed with 6 ng cDNA and Bio-Rad IQ SYBR Green Supermix (Bio-Rad CFX384 Touch Real Time PCR Detection System; Hercules, CA). Three independent biological replicates were collected at each time point, and each replicate contained six homogenized retinas from three fish (18 retinas/time point). Each biological replicate was run in triplicate. For each time point, average mRNA levels were represented as Log2 fold change, calculated using the DDC_T method and normalized to the housekeeping gene, *gpia*. Primers used for qPCR analyses are listed in Table 1.

Dexamethasone treatment

A previously described protocol was used that efficiently suppresses the immune system in zebrafish (Kyritsis et al., 2012; see also Bollaerts et al., 2019). Briefly, fish were housed in system water with 15 mg/L dexamethasone (Sigma-Aldrich, Corp, D1756) diluted in 0.1% MetOH. Dexamethasone-containing and control solutions were changed daily, and fish were fed brine shrimp every other day.

Immunohistochemistry

Tissues were fixed overnight at 4°C in 0.1M phosphate buffered 4% paraformaldehyde, cryoprotected with 20% sucrose, and embedded in optical cutting temperature (OCT) medium (Sakura Finetek USA, Torrance, CA). Immunohistochemistry (IHC) was performed as previously described (Taylor et al., 2015). Briefly, 10-μm-thick sections were collected such that the optic nerve head was included, and sections were mounted onto glass slides.

Sections were washed in phosphate buffer saline with 0.5% Triton-x (PBST) and incubated with 20% heat-inactivated normal sheep serum in PBST for 2 hours (NSS; Sigma-Aldrich, Corp.). Primary antibodies were applied overnight at 4°C. Sections were then washed with PBST and incubated in secondary antibodies for 1 hour at room temperature. Prior to IHC for BrdU, sections were immersed in 100°C sodium citrate buffer (10 mM sodium citrate, 0.05% Tween 20, pH 6.0) for 30 minutes and cooled at room temperature for 20 minutes. Sections were then subjected to IHC as described above.

Immunohistochemistry performed on whole retinas was conducted as described previously (Nagashima et al., 2017). Prior to IHC, retinas were dissected from dark-adapted animals, flattened with radial relaxing cuts, fixed at 4°C overnight in 4% paraformaldehyde in 0.1M phosphate buffer with 5% sucrose. Retinas were then placed in boiling sodium citrate buffer for 5 min and allowed to cool for 5 min. Retinas were incubated for 2 hours in 10% normal goat serum, 1% Tween, 1% Triton X-100, 1% DMSO, in phosphate buffered saline with 0.1% sodium azide. Primary and secondary antibody were diluted in 2% normal goat serum, 1% Tween, 1% Triton X-100, 1% DMSO, in phosphate buffered saline with 0.1% sodium azide and incubations were performed overnight at room temperature. After washing in phosphate buffered saline with 1% Tween, 1% Triton X-100, 1% DMSO, retinas were mounted on glass slides, photoreceptor side down, in ProLong Gold anti-fade reagent (Life Technologies Corp., Eugene, OR). Antibodies used in this study and their concentrations are listed in Table 2.

TUNEL staining

TUNEL staining was performed using *In Situ* Cell Death Detection Kit, TMR red (Sigma-Aldrich). Briefly, following immunocytochemistry, slides were treated with PBS containing 1% sodium citrate/ 1% TritonX-100 at 4°C, were rinsed with PBS, and them were incubated with TUNEL reaction cocktail for 30 min at 37°C.

Labeling dividing cells

In adults, dividing cells were labeled with BrdU by housing animals in system water containing 5 mM BrdU for 24 hours (Gramage et al., 2015).

In situ Hybridization

In situ hybridizations were performed as previously described (Luo et al., 2012). Digoxigenin (DIG)-labeled riboprobes for *rhodopsin* and *pde6c* were generated from full-length cDNA clones (Luo et al., 2012; Ochocinska and Hitchcock, 2007), whereas riboprobe for *mmp-9* was generated by PCR amplification using primers containing the T3 or T7 promoter sequences (David and Wedlich, 2001). *mmp-9* (F): 5’ TAATACGACTCACTATAGGGGATTCTTCTACTTCTGCCGGG 3’ *mmp-9* (R): 5’ AATTAACCCTCACTAAAGGGCTTAATAAATTTGTAAACAAG 3’.

Briefly, 10-μm-thick sections were hybridized with riboprobes at 55°C, incubated with an alkaline-phosphatase-conjugated anti-DIG antibody and visualized using Fast Red TR/ Naphthol AS-MX (SIGMA*FAST*) as the enzymatic substrate. When *in situ* hybridizations were combined with BrdU IHC, sections were removed from the fast red solutions, rinsed

and post-fixed in buffered 4% paraformaldehyde for 10 minutes then processed for BrdU IHC as described above.

Production of custom antibodies

Antibodies specific to zebrafish Mmp-9 were generated by Pocono Rabbit Farm & Laboratory (PRF&L, Canadensis, PA) as previously described (Calinescu et al., 2009). A 24 amino acid C-terminal peptide was used as the immunogen, CDIDGIQYLYGPRTGPEPTAPQPR; NCBI: AY151254. Polyclonal antibodies were affinity purified and confirmed by ELISA (data not shown). Western blots performed with retinal proteins using pre- and post-immune sera confirmed the post-immune serum detected a 76 kDa band, the predicted size for Mmp-9. Western blot analysis and known cleavage sites on pro-Mmp9 suggest these antibodies recognize both the pro- and active forms of Mmp-9, which can be distinguished by slight differences in their molecular weights (Vandooren et al., 2013a; see Results).

Western Blot Analysis

Protein samples were obtained from whole retinas homogenized in RIPA lysis buffer (ThermoFisher Scienific) containing protease and phosphatase inhibitor cocktail (5872S; Cell Signaling Technology, Danvers, MA, USA). Proteins were separated in a 12% Mini-PROTEAN TGX Precast gel (BioRad) and transferred to a polyvinylidene difluoride (PVDF) membrane (GenHunter Corp., Nashville, TN). To block non-specific staining, membranes were incubated in 5% nonfat dry milk in Tris buffered saline containing 0.3% Tween-20 (TBST) for 2 hours. Membranes were incubated with the antibodies-containing solution overnight at 4°C. Blots were then washed in TBST and incubated with horseradish peroxidase-conjugated secondary IgG (1:1000) for 1 hour at room temperature. Antibody-bound protein was visualized using Pierce ECL Western blotting substrate (32106; ThermoFisher Scienific, Waltham, MA). To visualize loading controls, blots were also stained with antibodies against actin. Images were captured using the Azure C500 (Azure Biosystems, Dublin, CA). Densitometry of protein bands was performed using ImageJ software (https://imagej.nih.gov/ij/).

Zymography

Protein samples were prepared as described for the Western blot analyses. Proteins were separated on 10% Zymogram Plus (Gelatin) Protein Gels, (ThermoFisher Scientific). Following electrophoresis, proteins were renatured in 1X renaturing buffer (ThermoFisher Scientific) for 30 mins at room temperature, then incubated in 1X developing buffer (ThermoFisher Scientific) overnight at 37º. Gels were rinsed in deionized water and stained with SimplyBlue SafeStain (ThermoFisher Scientific). Gels were imaged with long-wave ultraviolet light using the Azure C500 (Azure Biosystems; Dublin, CA). Active recombinant human MMP-9 (Calbiochem, San Diego, CA) was used as a positive control. Densitometry of the digested bands was performed using ImageJ software.

CRISPR-Cas9 mediated targeted mutation of Mmp-9

mmp-9 mutants were generated according to previously described methods (Hwang et al., 2013). ZiFiT software (available in the public domain at zifit.partners.org) was used to identify a 19bp sgRNA target sequence for *mmp-9* (GGCTGCTTCATGGCATCAA). Target sequence Oligo1- TTGATGCCATGAAGCAGCC and Oligo2- AAACTTGATGCCATGAAGCAG were annealed and subcloned into the pT7 gRNA vector (Addgene ID: 46759). The pCS2 nCas9n vector (Addgene ID: 46929) was used for Cas9 synthesis. To produce RNAs, the MEGAshortscript T7 kit (Ambion, Foster City, CA: AM1354) and mirVana miRNA Isolation kit (Ambion: AM 1560) were used for the gRNA, whereas, mMesage mMACHINE SP6 kit (Ambion: AM1340) and RNeasy mini Kit from (Qiagen: 74104) were used for the Cas9 mRNA. Single cell-stage embryos were injected with a 2nL solution containing 100 pg/nl sgRNA and 150 pg/nl Cas9 mRNA. Founders (F0) were outcrossed to AB wild-type fish. Mutations were identified using screening primers (F: 5′- AAGTCTGCAACTACATATCAGC −3′, R: 5′- GTACACACTGTAGATGCTGATAAG-3') that flanked the *mmp-9* sgRNA target site. Standard protocols for PCR used Platinum Taq-HF polymerase (Invitrogen) with genomic DNA as the template. The purified PCR product was subcloned into the pGEM-T Easy vector (Promega, Madison, WI) for Sanger sequencing. Mutant and wild-type sequences were aligned using pairwise blast (National Center for Biotechnology Information [NCBI], Bethesda, MD, USA). Premature stop codons were identified by comparing predicted amino acid sequences for wild-type and mutants using the ExPASy translate tool (available in the public domain at (www.expasy.org). F1 hybrids carrying a *mmp-9* mutation were in-crossed and homozygous F2 mutants were identified by a combination of Sanger sequencing and T7 endonuclease assays (New England Biolabs, Ipswich, MA) as previously described (www.crisprflydesign.org).

Imaging

Fluorescence images of retinal sections were captured using the Leica TCS SP5 confocal microscope (Leica Microsystems, Wetzlar, Germany). Cell counts were conducted using z-stack images and analyzed with Imaris software (Bitplane, South Windsor, CT). Regenerated photoreceptors were identified by the colocalization of DAPI, BrdU, and the ISH markers *pde6c* (cones) or *rho* (rods).

Cell Counts and area measurement.

Cells were counted in both radial sections and retinal wholemounts. In radial sections, cells were counted in three nonadjacent sections in each retina. The number of cells per retina were averaged, and averages were computed for control and experimental groups. In wholemounts stained with an antibody against the tight junction protein, ZO-1 (Nagashima et al., 2017), cones were identified in optical sections taken at the outer limiting membrane as profiles with perimeters greater than 3.5 μm. Cells were counted in five separate regions in each retina, sampling a totaling 5625μm^2 per retina. The average number of cells in control and experimental groups were then averaged.

Experimental Design and Statistical Analyses

The statistical significance in mRNA levels between unlesioned and lesioned retinas was calculated using an ANOVA (JMP 9.0; SAS Institute, Inc., Cary, NC). A p-value ≤ 0.05 was considered significant. The statistical significance in the number of cells between control and treated retinas was calculated using a student's t-test (GraphPad Prism Software, La Jolla, CA). A p-value ≤ 0.05 was considered significant. Western and zymogram analyses consisted of three independent biological replicates, and each replicate contained six homogenized retinas from three fish (18 retinas per time point). Statistical significance between optical density values of bands in control and experimental groups was calculated using an ANOVA (JMP 9.0, SAS Institute, Inc., Cary, NC). A p-value ≤ 0.05 was considered significant.

Results

Photoreceptor injury and death induce the expression of inflammatory genes

To characterize the inflammatory response during photoreceptor ablation and regeneration, qPCR was used to quantify the expression of inflammatory genes, *mmp-9, tnf−α*, *tnf-β*, *il-8, nfκb1,* and *nfκb2*, shown previously to regulate various forms of tissue regeneration in zebrafish (de Oliveira et al., 2013; LeBert et al., 2015; Nelson et al., 2013; Karra et al., 2015). The time course of gene expression follows closely the well-established time course for the injury response in Müller glia and the appearance and amplification of the Müller glia-derived progenitors and their subsequent differentiation into mature photoreceptors (Figure 1A; see (Gorsuch and Hyde, 2014)). Upregulation of gene expression can be detected by 8 hours post lesion (hpl), and the rising phase of expression corresponds to the period when Müller glia prepare to enter the cell cycle. Expression levels then slowly decline as the Müller glia-derived photoreceptor progenitors proliferate, migrate to the outer nuclear layer and differentiate (168 hpl; Figure 1A). Interestingly, among all the transcripts examined, *mmp-9* shows the greatest change from the undamaged controls, peaking at 24–48 hpl. Further, by 168 hpl *mmp-9* levels are reduced to only about 70% of the peak value (Figure 1A). The pro-inflammatory cytokine, Tnf−α, was shown to be responsible for initiating photoreceptor regeneration in zebrafish (Gorsuch and Hyde, 2014; Nelson et al., 2013), but at all time points in this assay, the levels of *tnf-α* expression were not significantly different from controls (also see below). Our assay for *tnf-α* failed to parallel the previous results (Nelson et al., 2013), and we infer this likely reflects the differences between the qPCR assay used here and the protein analysis used by Nelson et al. (2013). Nonetheless, these data show that in zebrafish photoreceptor death induces rapid expression of inflammatory genes that follows a time course reflecting the well-described events that underlie photoreceptor regeneration.

Inflammation regulates injury-induced proliferation and photoreceptor regeneration

To determine if inflammation regulates aspects of photoreceptor regeneration, the glucocorticoid steroid, dexamethasone (Dex), was used to suppress the inflammatory response. A 14-day pre-lesion treatment with Dex was chosen (Fig. 1B) based on studies performed by Kyritsis et al. (2012; see also White et al., 2017; Tsarouchas et al., 2018; Caldwell et al., 2019; Bollaerts et al., 2019), and here the dose of Dex, route of

administration and sizes and ages of animals were matched with Kyritis et al. (2012). Whereas this lengthy treatment with Dex may affect homeostatic function in all cells (Juszczak and Stankiewicz, 2018), this treatment in the absence of a lesion does not directly alter constitutive proliferation (SI Figure S1A; Kyritsis et al., 2012; White et al., 2017; Caldwell et al., 2019), the number of Müller glia or the expression and localization of *gfap*/Gfap, markers of reactive gliosis (SI Figure S1B-E). However, pretreatment with Dex does alter the morphology and the number of microglia (SI Figure S2A,B). Following Dex exposure microglia are less ramified (SI Figure S2A) and there are significantly fewer transgene/mCherry+ microglia detected in the Dex-treated retinas (SI Figure S2B). Further, in the Dex-treated animals, expression of the inflammatory cytokines, *tnfa*, *tnfb*, and the transcriptional regulators of inflammation, *nfkb1* and *nfkb2*, are significantly reduced (SI Figure S2C). These results indicate that Müller glia do not overtly respond to Dex-mediated immunosuppression, however pretreatment with Dex suppresses microglial reactivity and the expression of genes that underlie the inflammatory response. To validate the effectiveness of the Dex treatment following light lesion, the expression levels of inflammatory genes at 72 hpl, and the response of microglia and cell death were quantified in control and Dex-treated groups at 24 hpl. Compared with controls, the expression of *mmp-9*, *il-6*, and *nfκb1* were significantly decreased following Dex treatment (Figure 1C), while, though there was marked variability in the data, the expression of *tnf-α* and *il-8* were not significantly different from controls. Comparing the data in in Figures SI S2C and 1F suggest that Dex does not suppress the expression of *il-8*. Consistent with reports from larval zebrafish and chicken, Dex treatment suppresses the activation of microglia and their migration to the outer nuclear layer in response to photoreceptor death (Figure 1D, E; White et al., 2017; Gallina et al., 2015). However, Dex treatment does not alter the extent of photoreceptor cell death (Figure 1F), indicating that in zebrafish Dex is not neuroprotective.

Assays of proliferation and photoreceptor regeneration were performed for control animals and animals treated with Dex. Dividing cells were labelled with BrdU between 48 and 72 hpl to mark progenitors that will give rise to regenerated photoreceptors (Figure. 2A). To exclude proliferating microglia, BrdU-positive cells in the subretinal space were not counted. At 72 hpl, there was significantly fewer BrdU-labeled cells in Dex-treated retinas compared to controls (Figure 2B, C). At 7 dpl, there were significantly fewer regenerated rod and cone photoreceptors in Dex-treated groups compared to controls (Figure 2D-G). These results indicate that, consistent with data showing the requirement for inflammation in neuronal regeneration in the forebrain of zebrafish (Kyritsis et al., 2012), inflammatory mechanisms also promote photoreceptor regeneration in the retina.

Müller glia and Müller glia-derived progenitors express *mmp-9*

MMP-9 belongs to a large family of Zn^2+-dependent proteases that target a variety of substrates, such as extracellular matrix (ECM), growth factors, chemokines, and cytokines. Mmp-9 serves diverse functions among vertebrates (Pedersen et al. 2015; Page-McCaw, et al., 2007; Vandooren, 2013b; Iyer et al. 2012). Mmp-9 and Mmp-2 belong to the subfamily of gelatinases, and genes encoding both Mmp-9 and Mmp-2 are upregulated by photoreceptor death, though the induction of Mmp-9 is 10-times greater than Mmp-2 (Calinescu et al., 2009; (http://www.ncbi.nlm.nih.gov/geo/query/acc.cgi?acc=GSE13999;

data not shown). Due to the magnitude of its induction (Figure 1A) and the varied roles played by *mmp-9* in injured/regenerating tissues and inflammation (Vandooren et al., 2014), the specific function of Mmp-9 was investigated further. As a first step, *in situ* hybridization was performed to identify the cellular patterns of expression of *mmp-9*. This was undertaken using the Müller glia reporter line, *Tg[gfap:EGFP]mi2002* (Bernardos and Raymond, 2006), and BrdU labeling 24 hrs prior to sacrifice. By *in situ* hybridization, *mmp-9* is not detectable in unlesioned retinas. In contrast, by 24 hpl, *mmp-9* is expressed in Müller glia, and this time-point is prior to their entry into S-phase of the cell cycle (Figure 3A). By 48 hpl, ~97% of BrdU-labeled Müller glia express *mmp-9* (Figure 3A, B). At 72 hpl, the expression of *mmp-9* decreases (Figure 3A, C), and the cellular expression shifts to the Müller glia-derived progenitors, as evidenced by the absence of eGFP in the BrdU-labeled cells that express *mmp-9* (Figure 3A). The expression of *mmp-9* is also detected in very small number of microglia (data not shown). However, the majority of these cells reside in the subretinal space and were excluded from this analysis. These data indicated that photoreceptor ablation induces the expression of *mmp-9* in Müller glia, and this expression persists in Müller glia-derived progenitors. Further, these results suggest that *mmp-9* identifies that subset of Müller glia that enter the cell cycle in response to a retinal injury.

Mmp-9 protein is present and catalytically active following photoreceptor death

To characterize protein synthesis and catalytic activity, Western blot analysis and zymogram assays were used, respectively (Vandooren et al., 2013a, 2013b; Figure 4). By these assays, Mmp-9 is not detectable in unlesioned retinas, consistent with the *in situ* hybridization data (Figure 3A, 4A). In Western blots, at 16 hpl, the first time point sampled, Mmp-9 is present at very low levels (Figure 4A). Mmp-9 levels peak by 24 hpl, and then decrease between 24 and 72 hpl (Figure 4A, B). Mmp-9 was originally named gelatinase B, because its substrate, shared with Mmp-2, is denatured type-1 collagen (gelatin). In zymography, the polyacrylamide gel contains gelatin, and after protein renaturation and gelatin staining, areas of protease activity appear as clear, negatively-stained bands against the stained background (Chattopadhyay and Shubayev, 2009; Vandooren et al., 2013a). The same protein samples used for the Western blot analysis were used for zymography. Recombinant, active human MMP-9 was used as a positive control and shows strong catalytic activity as evidenced by a large negatively-stained band (Figure 4C). Unlesioned retinas contain no detectable Mmp-9 catalytic activity. In contrast, the catalytic activity parallels the data from the Western blot analysis (Figure 4C, D). Together, results from the Western blot and zymogram analyses show that catalytically-active Mmp-9 is induced by a lesion that selectively kills photoreceptors, and the time course of Mmp-9 synthesis and catalytic activity parallels the proliferative phase of photoreceptor regeneration.

CRISPR mutants lack Mmp-9 protein and catalytic activity

To investigate the function of *mmp-9* during photoreceptor regeneration, mutants were generated using CRISPR-Cas9 (Hwang et al., 2013), targeted to the *mmp-9* catalytic domain within exon 2 (Figure 5A). The 19 base sgRNA produced several alleles, two of which were bred to homozygosity and characterized further, a 23 bp deletion (designated *mi5003*; ZFIN, https://zfin.org/) and an 8 bp insertion (designated *mi5004*; ZFIN, https://zfin.org/), respectively (Figure 5B). Individuals from the two lines were crossed to create compound

heterozygotes to evaluate the potential for off target effects in either of the two independent lines (see next section). Each of the two *mmp-9* lines carries a mutation that results in a frameshift that predicts premature stop codons (SI Table 1). Retinas from mutants were characterized by Western blot analysis and zymography. Unlesioned retinas had no detectable Mmp-9 or catalytic activity (Figure 5C, D). As expected, following photoreceptor ablation, Mmp-9 protein and catalytic activity are present in wild-type retinas (Figure 5C, D). In contrast, there was trace Mmp-9 and catalytic activity in the *mi5004* line, but no detectable Mmp-9 or catalytic activity in *mi5003* line (Figure 5C, D). Based on these results, subsequent experiments were conducting using the *mi5003* line, though the basic observations reported here were confirmed in the *mi5004* line (data not shown) and the compound heterozygotes (see below).

In Mmp9 mutants, photoreceptor death results in overproduction of photoreceptor progenitors and regenerated photoreceptors

We first sought to determine if there were any differences in retinal development or adult starting points for the injury-induced proliferation in the *mmp-9* mutants. At 72 hpf, there were no differences between wildtype and the two mutant lines in the size of the eyes or degree of proliferation (SI Figure 3A, B), indicating early retinal development was not altered by the absence of Mmp9. Similarly, qualitative comparisons of adult retinas showed the appearance of wildtype and mutant retinas did not vary in any identifiable manner (SI Figure 4A). Finally, comparing the number of Müller glia and the number of mitotic progenitors, which support the persistent neurogenesis in adult retinas (Raymond et al., 2006), showed there were no quantitative differences between wild-type animals and the *mi5003* line in the number of Müller glia or the level of intrinsic cell proliferation (SI Figure 4B, C).

To determine the consequence of Mmp-9 loss-of-function on retinal regeneration, wild-type and mutant animals received photolytic lesions. Counts of TUNEL-labeled in cells in retinal sections showed there were no differences in the extent of cell death between WT and mutant animals (131.2±22.64 vs. 137.60 ±28.98 in 400μm; p=0.6787; n=6). At 1, 2, and 3 dpl, there were no obvious qualitative or quantitative differences in morphology and the number of microglia (data not shown). To evaluate the loss of Mmp-9 on proliferation, Müller glia-derived progenitors were labeled with BrdU between 48–72 hpl, and BrdU-labeled cells were counted at 72 hpl. Relative to wild-type animals, mutants had significantly more BrdU-labeled progenitors at 72 hpl (Figure 6A, B). This over production of the Müller glia-derived progenitors was also observed in the *mi5004* line (data not shown) and compound heterozygotes (SI Figure 4D), indicating that the hyperproliferation is a consequence of the loss of Mmp9 and is unlikely to result from off-target effects caused by the CRISPR-cas9 technique.

It is well established that Mmp-9 plays a role in tissue remodeling and cell migration (Page-McCaw et al., 2007). To determine if Mmp-9 loss-of-function altered the migration of Müller glia-derived progenitors from the inner nuclear layer to the outer nuclear layer, animals were subjected to photolytic lesions, exposed to BrdU between 48 and 72 hpl and allowed to survive to 7 dpl, a time point where proliferation and migration are complete and

photoreceptor differentiation has commenced. Qualitative inspection showed that Mmp-9 loss-of-function does not alter the migration of the Müller glia-derived progenitors (Figure 6C). Further, cell counts showed that the over production of photoreceptor progenitors observed in mutants at 72 hpl results in significantly more BrdU-labeled cells within the ONL at 7 dpl (Figure 6B, D). Finally, in the mutants at 7 dpl, there were significantly more regenerated rod and cone photoreceptors (Figure 6E-G). Together, these data show that, in the absence of an injury, Mmp-9 loss-of-function has no impact retinal development, the proliferative potential of the adult retina or the migration of Müller glia-derived progenitors following photoreceptor death. The hyperproliferation of the photoreceptor progenitors in mutants indicates that Mmp-9 functions as a negative regulator of proliferation among Müller glia-derived progenitors, though the mechanistic details through which this is accomplished are not yet known (see Discussion). Further, though over-produced, the presence of regenerated photoreceptors at 7 dpl indicates that Mmp-9 plays no apparent role in governing the timing of cell cycle exit or the onset of photoreceptor differentiation.

Absence of Mmp-9 results in elevated levels of *tnf−α*

MMP-9 can cleave inflammatory cytokines, and may modify cytokine signaling during the injury-induced proliferation (Parks et al., 2004; Aldo et al., 2018). To determine if the absence of MMP-9 results in an altered inflammatory response following photoreceptor death, we compared the expression of inflammatory genes in wildtype fish and mutants. In wildtypes, although the fold increase is less, the expression of *tnf-β* (Figure 7A), *nfκb1* (Figure 7B), *nfκb2* (Figure 7C), *il-8* (Figure 7D) and *tnf−α* (Figure 7E) follow similar temporal patterns as observed in Figure 1A. In mutants, the expression of *tnf-β*, *nfκb1, nfκb2* and *il-8* do not differ from wildtypes, with exception that in mutant retinas the initial induction of *il-8* was significantly reduced (Figure 7A-D). In contrast, in mutants the expression of *tnf−α* was significantly greater in both unlesioned retinas and lesioned retinas at all post-lesion time-points (Figure 7E). These data indicate that in the absence of Mmp-9, *tnf−α* levels are significantly elevated, and Mmp-9 negatively regulates the expression of *tnf −α* . In zebrafish Tnfα is necessary and sufficient to induce proliferation of Müller glia and Müller glia-derived progenitors (Nelson et al., 2013; Conner et al., 2014), and we infer that elevated levels of *tnf−α* in the Mmp9 mutants may account for the hyperproliferation among Müller glia-derived progenitors.

Mmp-9 is required for the survival of regenerated cone photoreceptors

To determine if in the mutants the initial overproduction of photoreceptors persists, regenerated rod and cone photoreceptors were qualitatively and quantitatively compared in wild-type and mutants at 21 dpl, a time point where regeneration is complete (Powell et al., 2016). For both groups, regenerated rod and cone photoreceptors were counted in sections and whole mount preparations. These analyses showed there were no qualitative differences between wild-type and mutants in the appearance of regenerated rod photoreceptors (Figure 8A), and the over production of rod photoreceptors observed at 7 dpl was present at 21 dpl (Figure 8B, C).

In contrast to the regenerated rods, in mutant retinas at 21 dpl, the survival of cones were markedly compromised. In mutants, regenerated cones had shorter outer segments and

appeared to be fewer in number (Figure 8A, insets 8B). Counts of regenerated cones in tissues sections showed the initial over production of cones, evident at 7 dpl, was absent at 21 dpl (Figure 8C). Cones were also counted in retinal whole mounts (Figure 9A, B). In both wild-type and mutant retinas, cone photoreceptors in unlesioned retinas are arranged in a very precise lattice mosaic, a feature of cone photoreceptors in teleost retinas (Nagashima et al., 2017; Figure 9A). There was no significant difference in the number of cone photoreceptors in unlesioned retinas from wild types and the mutants (Figure 9B). Following photoreceptor ablation and regeneration, areas of the retina that contain regenerated photoreceptors are identifiable by the marked spatial degradation of the mosaic, though individual cone photoreceptors remain readily identifiable (Nagashima et al., 2017). Counts of cones in whole mounts show that mutants had significantly fewer regenerated cones than wildtype animals (Figure 9A, B). Finally, as an independent measure of regenerated cones, Western blot analysis was performed using an antibody against Gnat-2 (transducin), a cone-specific protein (Figure 9C; Lagman et al., 2015). Gnat-2 levels in unlesioned retinas were comparable in wild-type and mutant animals. In lesioned retinas, Gnat-2 levels begin to recover in wild-type animals by 14 dpl, and by 21 dpl values in wild-type animals were nearly at the levels found in unlesioned retinas (Figure 9C, D). In contrast, Gnat-2 levels in mutants lagged behind wild-type levels, and at 21 dpl Gnat-2 levels in mutant animals were significantly less than in wild-types (Figure 9C, D). Western blot analysis using rhodopsin antibodies showed there were no differences in rod photoreceptors between wild-type and mutant animals (data not shown). Together, these results indicate that the absence of Mmp-9 results in defects specific to regenerated cone photoreceptors, well after injury-induced proliferation and the initial differentiation of regenerated photoreceptors is complete.

Immune suppression rescues regenerated cones in *mmp-9* mutants

MMP-9 can modify elements of the inflammatory response (see above; Parks et al., 2004). We hypothesized that the defects in the survival of cone photoreceptors in the Mmp-9 mutants is a consequence of an altered inflammatory milieu within the outer retina. Activated microglia are a hallmark of inflammation and are associated with retinal degenerative diseases (Madeira et al., 2015; Ma et al., 2015). For example, in rd10 mice, microglia phagocytose living photoreceptors, and genetic ablation of retinal microglia improves photoreceptor survival (Zhao et al., 2015; see also Gallina et al., 2014). Therefore, we first examined microglia in wildtype and mutant retinas. At 21 dpl, there were significantly more microglia in the mutant retinas (0.1 ± 0.3 cells/400μm, n=4 vs. 4 ± 2.2 cells/ 400 μm, n=4; p=0.0148; Figure 10A), suggesting that in the absence of Mmp-9 there is elevated inflammation following photoreceptor regeneration. To determine if immunosuppression rescues the defects in the survival of regenerated cones, we treated mutants with vehicle solution or Dex between 3 and 13 dpl. This treatment was started after the initial formation of Müller glia-derived progenitors and lasted throughout the phase of photoreceptor differentiation (Figure 10B). Relative to controls, in the retinas of Dex-treated mutants there were few microglia (Figure 10C), indicating that Dex treatment in the Mmp-9 mutant suppresses microglial activation. In the Dex-treated mutants, regenerated cones were longer and appeared more mature than cones in control retinas (Figure 10D). Finally, there were significantly more regenerated cones in the Dex-treated retinas than in the vehicle-treated retinas (Figure 10E, F), and Dex treatment restored the spatial pattern of regenerated

cones nearly to that observed in wild-type animals (Figure 9B; Figure 10E, F). These results suggest that following photoreceptor regeneration the absence of Mmp-9 results in an altered inflammatory environment within the outer retina, which selectively compromises the survival of cone photoreceptors. Further, our results suggest that in the regenerating retina microglia govern the survival regenerated photoreceptors.

Discussion

The results of this study are summarized in Figure 11. In response to photoreceptor death, Müller glia undergo a single asymmetric division through interkinetic nuclear migration to produce progenitors, which rapidly proliferate, migrate and differentiate to replace the ablated photoreceptors (Figure 11A, B). Dexamethasone-induced immunosuppression inhibits proliferation of Müller glia-derived progenitors, resulting in diminished photoreceptor regeneration (Figure 11C). Loss of Mmp-9 function results in hyperproliferation and overproduction of regenerated photoreceptors (Figure 11D). However, the absence of Mmp-9 leads to defects in the survival of cone photoreceptors (Figure 11D). Immunosuppression in mutants following photoreceptor regeneration rescues the survival defects (Figure 10E). Based on these results, we conclude that inflammation is required during the proliferative phase of photoreceptor regeneration, and Mmp-9 negatively regulates proliferation of Muller glia and their progenitors. Finally, we conclude that Mmp-9 is required for the survival of regenerated cone photoreceptors.

In the adult zebrafish, immune suppression using Dex inhibits the production of neural progenitors after a lesion (Kyritsis et al., 2012; Caldwell et al., 2019), and we show that treatment with Dex inhibits the proliferation of Müller glia-derived progenitors. Following a neurotoxic lesion in the retina of the chick, Dex inhibits proliferation of Müller glia-derived progenitors by activating glucocorticoid receptors on Müller glia (Gallina et al., 2014, 2015; see also Fischer et al., 2014). Our data suggest that Dex inhibits proliferation by altering the microglia response following photoreceptor death, however, we cannot exclude the possibility that in zebrafish Dex also acts directly on Müller glia or Müller glia-derived progenitors. Regardless of the mechanisms of action, our data showing that immune suppression inhibits photoreceptor regeneration are consistent with previous studies utilizing immune suppression in regeneration paradigms and indicate that acute inflammation is a required component of successful neuronal regeneration in the vertebrate central nervous system.

MMP-9 is a member of the gelatinases, which includes Mmp-2. In the chick retina, gelatinase activity is present in unlesioned retinas. Following NMDA damage, global gelatinase activity diminishes slowly as Müller glia-derived progenitors proliferate (Campbell et al., 2019). Selectively inhibiting Mmp-9 activity has no effect on the proliferative response, whereas inhibiting MMP-2 prior to damage or growth factor treatment potentiates proliferation. In the chick Mmp-2 is produced by oligodendrocytes and non-astrocyte inner retinal glia, a cell type unique to the chick. In contrast, in zebrafish, in the absence of a lesion, *mmp-2* and *mmp-9* are expressed at very low levels, and neuronal injury very rapidly induces the expression of Mmp-9 in Müller glia destined to enter the cell

cycle. The differences in gelatinase function in the chick and zebrafish, particularly within a tissue that is so highly evolutionarily conserved, is intriguing.

Mmp-9 loss-of-function results in hyperproliferation of Müller glia-derived progenitors, resulting initially in more regenerated photoreceptors. The overproduction of regenerated photoreceptors is interpreted simply to result from the overproduction of progenitors, and Mmp-9 plays no role in the timing of cell cycle exit or initial photoreceptor differentiation. There are at least three interpretations that explain the overproduction of photoreceptor progenitors. First, the absence of Mmp-9 may allow more Müller glia to enter the cell cycle. Previous studies showed that neuronal damage results in only 65–75% of the Müller glia entering the cell cycle (Nagashima et al., 2013). However, we demonstrated that *mmp-9* was expressed only by dividing Müller glia. The absence of proliferation in *mmp-9*-negative Müller glia argues against the possibility that additional Müller glia are recruited to the cell cycle. Second, in the *mmp-9* mutants Müller glia may undergo more than a one round of cell division, thereby increasing the size of the initial pool of Müller glia-derived progenitors, which then divide at a normal rate. We do not favor this possibility, given a single asymmetric division among Müller glia is a hallmark of regenerative neurogenesis in the zebrafish retina. Third, in the *mmp-9* mutants, proliferation of the Müller glia-derived progenitors is accelerated. We view this the likeliest of the three possibilities, and propose that, as an extracellular protease, Mmp-9 regulates the concentration of cytokines and/or growth factors that regulate cell cycle kinetics within the niche of progenitors that cluster around each parental Müller glia, and in the absence of Mmp-9, mitogenic signals persist, leading to accelerated proliferation (Bosak et al., 2018; Le et al., 2007; Manicone and Mcguire, 2008; Parks et al., 2004; Luo et al., 2012; Vandooren et al., 2013b). Tnf-α functions to activate proliferation among Müller glia and Müller glia-derived progenitors during photoreceptor regeneration (Nelson et al., 2013). Our qPCR data showing elevated *tnf-α* in the mutants is consistent with the possibility that in the absence of Mmp-9 elevated levels of active Tnf-α accelerate proliferation of Müller glia-derived progenitors. However, additional studies will be required to determine if Tnf-α is a direct catalytic substrate of Mmp-9 and the mechanisms by which the *tnf-α* transcript is regulated by this extracellular protease.

We show that immune suppression significantly suppresses *mmp-9* expression. This result is consistent with the literature indicating that Mmp-9 is a component of the neuroinflammatory response. Following neuronal death, Müller glia secrete the inflammatory cytokines, *tnf-α*, *leptin*, and *il-11* (Nelson et al., 2013; Zhao et al., 2014). Recent transcriptome and gene ontology analysis for isolated Müller glia, isolated during photoreceptor injury and death, identified cytokine signaling and the immune response as activated pathways (Roesch et al., 2012; Sifuentes et al., 2016). In the mammalian retina, neuronal death leads to persistent active gliosis in Müller glia and failure of the spontaneous expression of intrinsic reprogramming factors. This limits the ability for neuronal regeneration (Bringmann et al., 2006, 2009; Reichenbach and Bringmann, 2013; see also Ueki et al., 2015). Our data provide additional support that the innate immune response in the retina is required for stem cell-based neuronal regeneration. It is interesting to note that the activation of cytokine pathways is conserved in the transcriptomes of Müller glia in both zebrafish and mouse models of photoreceptor degeneration (Roesch et al., 2012; Sifuentes et

al., 2016), suggesting that photoreceptor death in vertebrates results in a common inflammatory response among Müller glia.

Recently, Kaur et al (2018) demonstrated a regulatory feedback loop involving Shh and Mmp-9 during retinal regeneration in zebrafish. They found that *mmp-9* is rapidly induced by a retinal injury, and pharmacological and genetic suppression of Shh signaling caused a significant upregulation in *mmp-9* and inhibited proliferation of Müller glia-derived progenitors. The hyperproliferation we observed in the *mmp-9* mutants, and the conclusion that Mmp-9 negatively regulates proliferation of Müller glia-derived progenitors, is consistent with their data. Kaur et al. (2018) also show there is a positive feedback loop between Shh signaling pathways and Mmp-9, suggesting that Shh may be a proteolytic substrate for the Mmp-9. However, Kauer et al., (2018) also report that pharmacological and morpholino-based inhibition of Mmp-9 decreases the production of Müller glia-derived progenitors. This latter observation is inconsistent with our data and raises the possibility that differences in technical approaches or injury paradigms (retinal stab wounds result in bloodborne factors and cells invading the retina (see White et al., 2017), may account for differences in our respective data.

White et al, (2017) showed that in larval zebrafish the timing of immune suppression can delay or accelerate the regeneration of rod photoreceptors. As a pre-treatment, dexamethasone suppresses the regeneration of rods. This result aligns with what we report here for adults - inflammatory events are required for the activation of Müller glia and proliferation of Müller glia-derived progenitors. However, if dexamethasone treatment commences after rod photoreceptor ablation, regeneration kinetics are enhanced. The enhanced regeneration following delayed immune suppression parallels the results from the Mmp-9 mutants, but it is unlikely a common mechanism can readily account for both results. The molecular milieu is complex in injured tissues, and the potential parallels between delayed suppression of inflammation and the absence of Mmp-9 await further characterization.

We found that in the Mmp-9 loss-of-function mutants, the survival of regenerated cone photoreceptors is compromised. It is well established that chronic inflammation is a risk factor for photoreceptor dystrophies in humans, such as retinitis pigmentosa and age-related macular degeneration (AMD; Kauppinen et al., 2016; Chen and Xu, 2012; Whitcup et al., 2013; Yoshida et al., 2013). A subset of patients with AMD exhibit single nucleotide polymorphism (SNP) variants in the *MMP-9* gene, and elevated inflammation is associated with AMD pathogenesis (Fritsche et al., 2016; Kauppinen et al., 2016; Parks et al., 2004). Mutational variants in the inflammatory regulators, TIMP-3, TGFB, TNF-α are also identified in human patients with AMD (Fritsche et al., 2016). We hypothesize that during photoreceptor regeneration in zebrafish, Mmp-9 function is required to modulate inflammation activated by the death of photoreceptors, and, in the *mmp-9* mutants, there an altered inflammatory environment that is selectively damaging to cones. The *mmp-9* mutants studied here may recapitulate elements of the pathologies that are characteristic of inflammatory photoreceptor diseases in humans, including AMD. Our study begins to shed light on the functional roles of Mmp-9 in the retina and a potentially important link between intrinsic retinal immunity, human photoreceptor dystrophies and photoreceptor regeneration.

Supplementary Material

Refer to Web version on PubMed Central for supplementary material.

Acknowledgements:

This work was supported by grants from the National Institutes of Health - R01EY07060 (PFH), T32EY013934 (NJS), P30EYO7003 (PFH), R01 EY024519 (DRH), U01EY027267 (DRH), and an unrestricted grant from the Research to Prevent Blindness, New York. The authors thank Dilip Pawar for technical assistance. Fish lines and reagents provided by ZIRC were supported by NIH-NCRR Grant P40 RR01.

References

Amor S, Puentes F, Baker D, van der Valk P. 2010 Inflammation in neurodegenerative diseases. Immunology 129:154–169. [PubMed: 20561356]

Ando K, Shibata E, Hans S, Brand M, Kawakami A. 2017 Osteoblast Production by Reserved Progenitor Cells in Zebrafish Bone Regeneration and Maintenance. Dev Cell 43:643–650.e3. [PubMed: 29103952]

Bernardos RL, Barthel LK, Meyers JR, Raymond PA. 2007 Late-stage neuronal progenitors in the retina are radial Müller glia that function as retinal stem cells. J Neurosci 27:7028–7040. [PubMed: 17596452]

Bernardos RL, Raymond PA. 2006 GFAP transgenic zebrafish. Gene Expr Patterns 6:1007–1013. [PubMed: 16765104]

Bollaerts I, Van Houcke J, Beckers A, Lemmens K, Vanhunsel S, De Groef L, Moons L. 2019 Prior Exposure to Immunosuppressors Sensitizes Retinal Microglia and Accelerates Optic Nerve Regeneration in Zebrafish. Mediators Inflamm. Article ID:6135795.

Bonnans C, Chou J, Werb Z. 2014 Remodelling the extracellular matrix in development and disease. Nat Rev Mol Cell Biol 15:786–801. [PubMed: 25415508]

Borsini A, Zunszain PA, Thuret S, Pariante CM. 2015 The role of inflammatory cytokines as key modulators of neurogenesis. Trends Neurosci 38:145–157. [PubMed: 25579391]

Bosak V, Murata K, Bludau O, Brand M. 2018 Role of the immune response in initiating central nervous system regeneration in vertebrates: learning from the fish. Int J Dev Biol 62:403–417. [PubMed: 29938753]

Bringmann A, Pannicke T, Grosche J, Francke M, Wiedemann P, Skatchkov SN, Osborne NN, Reichenbach A. 2006 Müller cells in the healthy and diseased retina. Prog Retin Eye Res 25:397–424. [PubMed: 16839797]

Bringmann A, Iandiev I, Pannicke T, Wurm A, Hollborn M, Wiedemann P, Osborne NN, Reichenbach A. 2009 Cellular signaling and factors involved in Müller cell gliosis: neuroprotective and detrimental effects. Prog Retin Eye Res 28:423–451. [PubMed: 19660572]

Campbell WA, Deshmukh A, Blum S, Todd L, Mendonca N, Weist J, Zent J, Hoang TV Blackshaw S, Leight J, Fischer AJ. 2019 Matrix-metalloproteinase expression and gelatinase activity in the avian retina and their influence on Müller glia proliferation. Experimental Neurology. 0014–4886.

Caldwell LJ, Davies NO, Cavone L, Mysiak KS, Semenova SA, Panula P, Armstrong JD, Becker CG, Becker T. 2019 Regeneration of dopaminergic neurons in adult zebrafish depends on immune system activation and differs for distinct populations. J Neurosci., 8

Calinescu A-A, Raymond PA, Hitchcock PF. 2009 Midkine expression is regulated by the circadian clock in the retina of the zebrafish. Vis Neurosci 26:495–501. [PubMed: 19860997]

Chattopadhyay S, Shubayev VI. 2009 MMP-9 controls Schwann cell proliferation and phenotypic remodeling via IGF-1 and ErbB receptor-mediated activation of MEK/ERK pathway. Glia 57:1316–1325. [PubMed: 19229995]

Chen M, Xu H. 2012 Inflammation in Age-Related Macular Degeneration – Implications for Therapy, Inflammatory Diseases - Immunopathology, Clinical and Pharmacological Bases (Khatami Mahin, ed), pp. 129–150. IntechOpen, DOI: 10.5772/25658.

David R, Wedlich D. 2001 PCR-based RNA probes: a quick and sensitive method to improve whole mount embryo in situ hybridizations. Biotechniques 30:769–72, 74. [PubMed: 11314259]

De Oliveira S, Reyes-Aldasoro CC, Candel S, Renshaw SA, Mulero V, Calado A. 2013 Cxcl8 (IL-8) mediates neutrophil recruitment and behavior in the zebrafish inflammatory response. J Immunol 190:4349–4359. [PubMed: 23509368]

Deverman BE, Patterson PH. 2009 Cytokines and CNS Development. Neuron 64:61–78. [PubMed: 19840550]

Ekdahl CT, Kokaia Z, Lindvall O. 2009 Brain inflammation and adult neurogenesis: the dual role of microglia. Neuroscience 158:1021–1029. [PubMed: 18662748]

Ellett F, Pase L, Hayman JW, Andrianopoulos A, Lieschke GJ. 2011 mpeg1 promoter transgenes direct macrophage-lineage expression in zebrafish. Blood. 117(4):e49–56. [PubMed: 21084707]

Fausett BV, Goldman D. 2006 A role for alpha1 tubulin-expressing Müller glia in regeneration of the injured zebrafish retina. J Neurosci 26:6303–6313. [PubMed: 16763038]

Fimbel SM, Montgomery JE, Burket CT, Hyde DR. 2007 Regeneration of inner retinal neurons after intravitreal injection of ouabain in zebrafish. J Neurosci. 14:1712–24.

Fischer AJ, Zelinka C, Gallina D, Scott MA, Todd L. 2014 Reactive microglia and macrophage facilitate the formation of Müller glia-derived retinal progenitors. Glia 62:1608–1628. [PubMed: 24916856]

Fritsche LG, Igl W, Bailey JNC, Grassmann F, Sengupta S, Bragg-Gresham JL, Burdon KP, Hebbring SJ, Wen C, Gorski M, Kim IK, Cho D, Zack D, Souied E, Scholl HPN, Bala E, Lee KE, Hunter DJ, Sardell RJ, Mitchell P, Merriam JE, Cipriani V, Hoffman JD, Schick T, Lechanteur YTE, Guymer RH, Johnson MP, Jiang Y, Stanton CM, Buitendijk GHS, Zhan X, Kwong AM, Boleda A, Brooks M, Gieser L, Ratnapriya R, Branham KE, Foerster JR, Heckenlively JR, Othman MI, Vote BJ, Liang HH, Souzeau E, McAllister IL, Isaacs T, Hall J, Lake S, Mackey DA, Constable IJ, Craig JE, Kitchner TE, Yang Z, Su Z, Luo H, Chen D, Ouyang H, Flagg K, Lin D, Mao G, Ferreyra H, Stark K, von Strachwitz CN, Wolf A, Brandl C, Rudolph G, Olden M, Morrison MA, Morgan DJ, Schu M, Ahn J, Silvestri G, Tsironi EE, Park KH, Farrer LA, Orlin A, Brucker A, Li M, Curcio CA, Mohand-Saïd S, Sahel J-A, Audo I, Benchaboune M, Cree AJ, Rennie CA, Goverdhan SV, Grunin M, Hagbi-Levi S, Campochiaro P, Katsanis N, Holz FG, Blond F, Blanché H, Deleuze J-F, Igo RP Jr, Truitt B, Peachey NS, Meuer SM, Myers CE, Moore EL, Klein R, Hauser MA, Postel EA, Courtenay MD, Schwartz SG, Kovach JL, Scott WK, Liew G, Tan AG, Gopinath B, Merriam JC, Smith RT, Khan JC, Shahid H, Moore AT, McGrath JA, Laux R, Brantley MA Jr, Agarwal A, Ersoy L, Caramoy A, Langmann T, Saksens NTM, de Jong EK, Hoyng CB, Cain MS, Richardson AJ, Martin TM, Blangero J, Weeks DE, Dhillon B, van Duijn CM, Doheny KF, Romm J, Klaver CCW, Hayward C, Gorin MB, Klein ML, Baird PN, den Hollander AI, Fauser S, Yates JRW, Allikmets R, Wang JJ, Schaumberg DA, Klein BEK, Hagstrom SA, Chowers I, Lotery AJ, Léveillard T, Zhang K, Brilliant MH, Hewitt AW, Swaroop A, Chew EY, Pericak-Vance MA, DeAngelis M, Stambolian D, Haines JL, Iyengar SK, Weber BHF, Abecasis GR, Heid IM. 2016 A large genome-wide association study of age-related macular degeneration highlights contributions of rare and common variants. Nat Genet 48:134–143. [PubMed: 26691988]

Gallina D, Zelinka C, and Fischer A. 2014 Glucocorticoid receptors in the retina, Müller glia and the formation of Müller glia-derived progenitors. Development 3340–3351. [PubMed: 25085975]

Gallina D, Zelinka CP, Cebulla CM, Fischer. 2015 Activation of glucocorticoid receptors in Müller glia is protective to retinal neurons and suppresses microglial reactivity. Exp Neurol 273:114–125. [PubMed: 26272753]

Gemberling M, Bailey TJ, Hyde DR, Poss KD. 2013 The zebrafish as a model for complex tissue regeneration. Trends Genet 29:611–620. [PubMed: 23927865]

Goldman D. 2014 Müller glial cell reprogramming and retina regeneration. Nat Rev Neurosci 15:431–442. [PubMed: 24894585]

Gorsuch RA, Hyde DR. 2014 Regulation of Müller glial dependent neuronal regeneration in the damaged adult zebrafish retina. Exp Eye Res 123:131–140. [PubMed: 23880528]

Gramage E, D'Cruz T, Taylor S, Thummel R, Hitchcock PF. 2015 Midkine-a Protein Localization in the Developing and Adult Retina of the Zebrafish and Its Function During Photoreceptor Regeneration. PLoS One 10:e0121789. [PubMed: 25803551]

Hindi SM, Shin J, Ogura Y, Li H, Kumar A. 2013 Matrix Metalloproteinase-9 Inhibition Improves Proliferation and Engraftment of Myogenic Cells in Dystrophic Muscle of mdx Mice. PLoS One 8:e72121. [PubMed: 23977226]

Hwang WY, Fu Y, Reyon D, Maeder ML, Tsai SQ, Sander JD, Peterson RT, Yeh J-RJ, Keith Joung J. 2013 Efficient genome editing in zebrafish using a CRISPR-Cas system. Nat Biotechnol 31:227–229. [PubMed: 23360964]

Iyer RP, Nicolle LP, Gregg BF, Merry LL. 2012 The History of Matrix Metalloproteinases: Milestones, Myths, and Misperceptions. American Journal of Physiology. 303: H919–30. [PubMed: 22904159]

Juszczak GR, Stankiewicz AM. 2018 Glucocorticoids, genes and brain function. Prog Neuropsychopharmacol Biol Psychiatry. 82:136–168. [PubMed: 29180230]

Karra R, Knecht AK, Kikuchi K, Poss KD. 2015 Myocardial NF-κB activation is essential for zebrafish heart regeneration. Proc Natl Acad Sci U S A 112:13255–13260. [PubMed: 26472034]

Kauppinen A, Paterno JJ, Blasiak J, Salminen A, Kaarniranta K. 2016 Inflammation and its role in age-related macular degeneration. Cell Mol Life Sci 73:1765–1786. [PubMed: 26852158]

Kaur S, Gupta S, Chaudhary M, Khursheed MA, Mitra S, Kurup AJ, Ramachandran R. 2018 let-7 MicroRNA-Mediated Regulation of Shh Signaling and the Gene Regulatory Network Is Essential for Retina Regeneration. Cell Rep 23:1409–1423. [PubMed: 29719254]

Kizil C, Kaslin J, Kroehne V, Brand M. 2012 Adult neurogenesis and brain regeneration in zebrafish. Dev Neurobiol 72:429–461. [PubMed: 21595047]

Kizil C, Kyritsis N, Brand M. 2015 Effects of inflammation on stem cells: together they strive? EMBO Rep 16:416–426. [PubMed: 25739812]

Kyritsis N, Kizil C, Brand M. 2014 Neuroinflammation and central nervous system regeneration in vertebrates. Trends Cell Biol 24:128–135. [PubMed: 24029244]

Kyritsis N, Kizil C, Zocher S, Kroehne V, Kaslin J, Freudenreich D, Iltzsche A, Brand M. 2012 Acute inflammation initiates the regenerative response in the adult zebrafish brain. Science 338:1353–1356. [PubMed: 23138980]

Lagman D, Callado-Pérez A, Franzén IE, Larhammar D, Abalo XM. 2015 Transducin duplicates in the zebrafish retina and pineal complex: differential specialisation after the teleost tetraploidisation. PLoS One. 10:e0121330. [PubMed: 25806532]

LeBert DC, Squirrell JM, Rindy J, Broadbridge E, Lui Y, Zakrzewska A, Eliceiri KW, Meijer AH, Huttenlocher A. 2015 Matrix metalloproteinase 9 modulates collagen matrices and wound repair. Development 142:2136–2146. [PubMed: 26015541]

Lenkowski JR, Raymond PA. 2014 Müller glia: Stem cells for generation and regeneration of retinal neurons in teleost fish. Prog Retin Eye Res 40:94–123. [PubMed: 24412518]

Le NTV, Xue M, Castelnoble LA, Jackson CJ. 2007 The dual personalities of matrix metalloproteinases in inflammation. Front Biosci 12:1475–1487. [PubMed: 17127395]

Liddiard K, Rosas M, Davies LC, Jones SA, Taylor PR. 2011 Macrophage heterogeneity and acute inflammation. Eur J Immunol 41:2503–2508. [PubMed: 21952806]

Luo J, Uribe RA, Hayton S, Calinescu A-A, Gross JM, Hitchcock PF. 2012 Midkine-A functions upstream of Id2a to regulate cell cycle kinetics in the developing vertebrate retina. Neural Dev 7:33. [PubMed: 23111152]

Ma W, Lian Zhao L, Wong WT. 2011 Microglia in the Outer Retina and Their Relevance to Pathogenesis of Age-Related Macular Degeneration. Retinal Degenerative Diseases, pp 37–42.

Madeira MH, Boia R, Santos PF, Ambrósio AF, Santiago AR. 2015 Contribution of Microglia-Mediated Neuroinflammation to Retinal Degenerative Diseases. Mediators of Inflammation Vol. 2015, Article ID 673090.

Manicone A, Mcguire J. 2008 Matrix metalloproteinases as modulators of inflammation. Semin Cell Dev Biol 19:34–41. [PubMed: 17707664]

Martin JF, Poché RA. 2019 Awakening the Regenerative Potential of the Mammalian Retina. Development 146:1–6.

Masure S, Proost P, Van Damme J, Opdenakker G. 1991 Purification and identification of 91-kDa neutrophil gelatinase. Release by the activating peptide interleukin-8. Eur J Biochem 198:391–398. [PubMed: 1645657]

Nagase H, Visse R, Murphy G. 2006 Structure and Function of Matrix Metalloproteinases and TIMPs. Cardiovascular Research 69: 562–73. [PubMed: 16405877]

Nagashima M, Barthel LK, Raymond PA. 2013 A self-renewing division of zebrafish Müller glial cells generates neuronal progenitors that require N-cadherin to regenerate retinal neurons. Development 140:4510–4521. [PubMed: 24154521]

Nagashima M, Hadidjojo J, Barthel LK, Lubensky DK, Raymond PA. 2017 Anisotropic Müller glial scaffolding supports a multiplex lattice mosaic of photoreceptors in zebrafish retina. Neural Dev 12:20. [PubMed: 29141686]

Nathan C. 2002 Points of control in inflammation. Nature 420:846–852. [PubMed: 12490957]

Nelson CM, Ackerman KM, O'Hayer P, Bailey TJ, Gorsuch RA, Hyde DR. 2013 Tumor necrosis factor-alpha is produced by dying retinal neurons and is required for Muller glia proliferation during zebrafish retinal regeneration. J Neurosci 33:6524–6539. [PubMed: 23575850]

Ochocinska MJ, Hitchcock PF. 2007 Dynamic expression of the basic helix-loop-helix transcription factor neuroD in the rod and cone photoreceptor lineages in the retina of the embryonic and larval zebrafish. J Comp Neurol 501:1–12. [PubMed: 17206615]

Opdenakker G, Masure S, Proost P, Billiau A, van Damme J. 1991 Natural Human Monocyte Gelatinase and Its Inhibitor. FEBS Letters 284: 73–78. [PubMed: 1647974]

Page-McCaw A, Andrew JE, Zena W. 2007 "Matrix Metalloproteinases and the Regulation of Tissue Remodelling." Nature Reviews. Molecular Cell Biology 8: 221–33. [PubMed: 17318226]

Parks WC, Wilson CL, López-Boado YS. 2004 Matrix metalloproteinases as modulators of inflammation and innate immunity. Nat Rev Immunol 4:617–629. [PubMed: 15286728]

Pedersen ME, Tram TV, Sissel BR, Svein OK. 2015 Matrix Metalloproteinases in Fish Biology and Matrix Turnover. J Int Soc Matrix Biol. 44–46: 86–93.

Powell C, Cornblath E, Elsaeidi F, Wan J, Goldman D. 2016 Zebrafish Müller glia-derived progenitors are multipotent, exhibit proliferative biases and regenerate excess neurons. Sci Rep 6:24851. [PubMed: 27094545]

Raymond PA, Barthel LK, Bernardos RL, Perkowski JJ. 2006 Molecular characterization of retinal stem cells and their niches in adult zebrafish. BMC Dev Biol 6:36. [PubMed: 16872490]

Reichenbach A, Bringmann A. 2013 New functions of Müller cells. Glia 61:651–678. [PubMed: 23440929]

Roesch K, Stadler MB, Cepko CL. 2012 Gene expression changes within Müller glial cells in retinitis pigmentosa. Mol Vis 18:1197–1214. [PubMed: 22665967]

Sherpa T, Fimbel SM, Mallory DE, Maaswinkel H, Spritzer SD, Sand JA, Li L, Hyde DR, Stenkamp DL. 2008 Ganglion cell regeneration following whole-retina destruction in zebrafish. Dev Neurobiol. 68:166–81. [PubMed: 18000816]

Shubayev VI, Angert M, Dolkas J, Marie Campana W, Palenscar K, Myers RR. 2006 TNFα-induced MMP-9 promotes macrophage recruitment into injured peripheral nerve. Mol Cell Neurosci 31:407–415. [PubMed: 16297636]

Sifuentes CJ, Kim J-W, Swaroop A, Raymond PA. 2016 Rapid, Dynamic Activation of Müller Glial Stem Cell Responses in Zebrafish. Invest Ophthalmol Vis Sci 57:5148–5160. [PubMed: 27699411]

Taylor SM, Alvarez-Delfin K, Saade CJ, Thomas JL, Thummel R, Fadool JM, Hitchcock PF. 2015 The bHLH Transcription Factor NeuroD Governs Photoreceptor Genesis and Regeneration Through Delta-Notch Signaling. Invest Ophthalmol Vis Sci 56:7496–7515. [PubMed: 26580854]

Tsarouchas TM, Wehner D, Cavone L, Munir T, Keatinge M, Lamvertus M, Underhill A, Barrett Kassapis E, Ogryzko N, Feng Y, Van Ham TJ, Becker T, and Becker CG. 2018 Dynamic Control of proinflammatory cytokines il-1β and Tnf-α by macrophages in zebrafish spinal cord regeneration. Nature Comm. S41467–018-07036-w

Thomas JL, Ranski AH, Morgan GW, Thummel R. 2016 Reactive gliosis in the adult zebrafish retina. Exp Eye Res. 143:98–109. [PubMed: 26492821]

Ueki Y, Wilken MS, Cox KE, Chipman L, Jorstad N, Sternhagen K, Simic M, Ullom K, Nakafuku M, Reh TA. 2015 Transgenic expression of the proneural transcription factor Ascl1 in Müller glia stimulates retinal regeneration in young mice. Proc Nat Acad Sci 112:13737–13722.

Vandooren J, Geurts N, Martens E, Van den Steen PE, Opdenakker G. 2013a Zymography methods for visualizing hydrolytic enzymes. Nat Methods 10:211–220. [PubMed: 23443633]

Vandooren J, Van den Steen PE, Opdenakker G. 2013b Biochemistry and molecular biology of gelatinase B or matrix metalloproteinase-9 (MMP-9): the next decade. Crit Rev Biochem Mol Biol 48:222–272. [PubMed: 23547785]

Vandooren J, Van Damme J, Opdenakker G. 2014 On the structure and functions of gelatinase B/matrix metalloproteinase-9 in neuroinflammation. Prog Brain Res 214:193–206. [PubMed: 25410359]

Vecil GG, Larsen PH, Corley SM, Herx LM, Besson A, Goodyer CG, Yong VW. 2000 Interleukin-1 is a key regulator of matrix metalloproteinase-9 expression in human neurons in culture and following mouse brain trauma in vivo. J Neurosci Res 61:212–224. [PubMed: 10878594]

Whitcup SM, Nussenblatt RB, Lightman SL, Hollander DA. 2013 Inflammation in Retinal Disease. Int J Inflam 2013:1–4.

White DT, Sengupta S, Saxena MT, Xu Q, Hanes J, Ding D, Ji H, Mumm JS. 2017 Immunomodulation-accelerated neuronal regeneration following selective rod photoreceptor cell ablation in the zebrafish retina. Proc Nat Acad Sci 114:E3719–E3728. [PubMed: 28416692]

Xue Q, Cao L, Chen X-Y, Zhao J, Gao L, Li S-Z, Fei Z. 2017 High expression of MMP9 in glioma affects cell proliferation and is associated with patient survival rates. Oncol Lett 13:1325–1330. [PubMed: 28454256]

Yoshida N, Ikeda Y, Notomi S, Ishikawa K, Murakami Y, Hisatomi T, Enaida H, Ishibashi T. 2013 Laboratory evidence of sustained chronic inflammatory reaction in retinitis pigmentosa. Ophthalmology 120:e5–12.

Zhao L, Zabel M, Wang X, Ma W, Shah P, Fariss RN, Qian H, Parkhurst CN, Gan WB, Wong WT. 2015 Microglial phagocytosis of living photoreceptors contributes to inherited retinal degeneration. EMBO. 7(9), 1179–1197

Zhao X-F, Wan J, Powell C, Ramachandran R, Myers MG, Goldman D. 2014 Leptin and IL-6 Family Cytokines Synergize to Stimulate Müller Glia Reprogramming and Retina Regeneration. Cell Rep 9:272–284. [PubMed: 25263554]

Main Points:

- Acute inflammation is necessary for photoreceptor regeneration in zebrafish.
- MMP-9 negatively regulates Müller glia-derived progenitors during photoreceptor regeneration.
- Mmp-9 promotes the survival of regenerated cone photoreceptors.

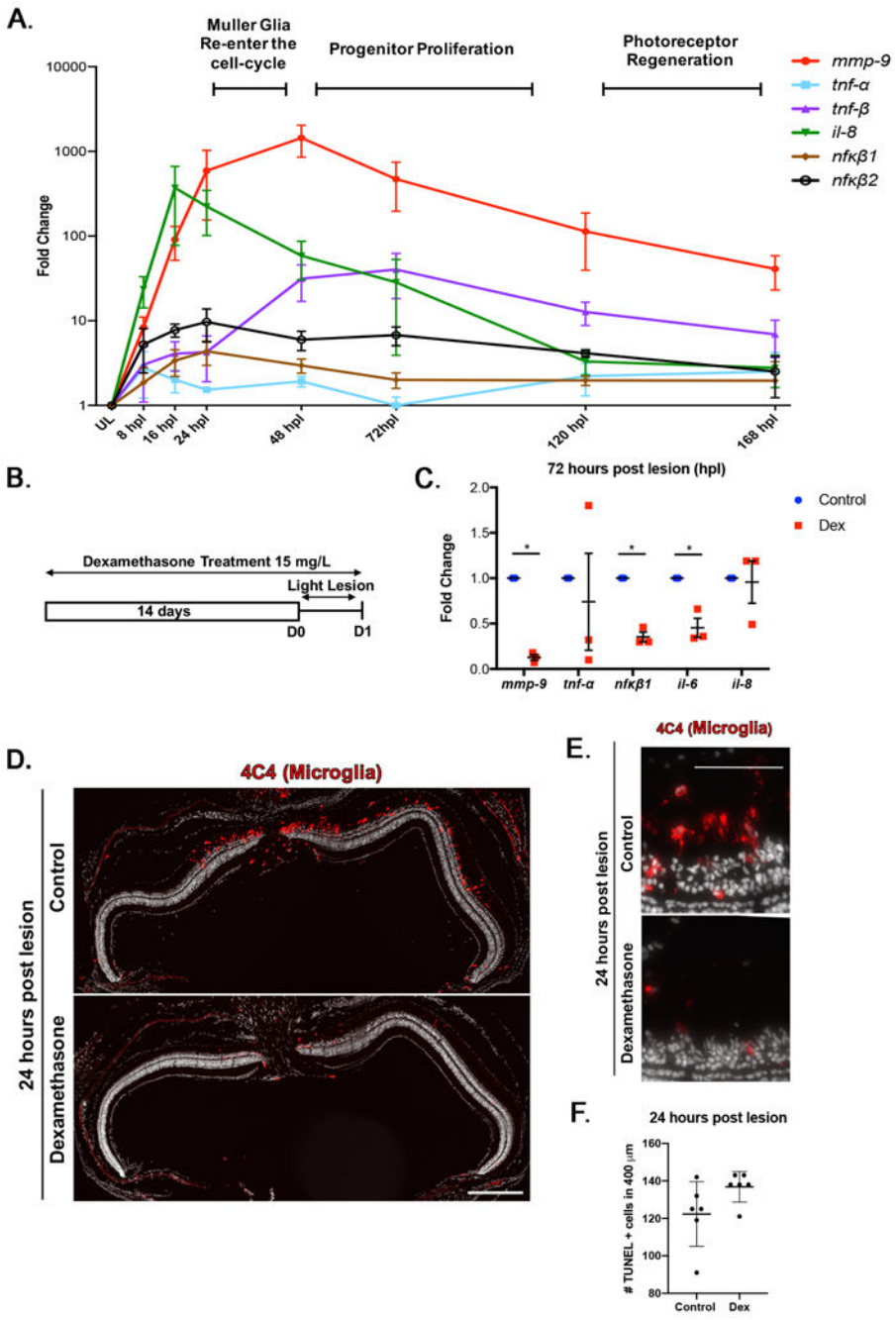

Figure 1: Inflammation is induced following photoreceptor ablation, Dexamethasone treatment suppresses microglia activation and cytokine production, but not photoreceptor death.

(A) Time-course for the expression of inflammatory genes, from 8 to 168 hours post lesion (hpl). Unlesioned retinas served as controls. Expression levels are represented as fold change calculated using DDC_T method. **(B)** Experimental paradigm for the immune suppression and BrdU labeling. **(C)** qRT-PCR for the inflammatory genes *mmp-9* (ANOVA F-ratio = 22.237, p<.0001), *tnf-α* (ANOVA F-ratio = 1.5507, p =.2209), *tnf-β* (ANOVA F-ratio = 6.5120, p =.001), *il-8* (ANOVA F-ratio = 8.2296, p =.0003), *nfκb1* (ANOVA F-ratio = 2.5207, p =.0596), and *nfκb2* (ANOVA F-ratio = 3.5591, p =.0168) from control and Dex-treated

retinas at 72 hpl. *p≤0.05. **(D)** Immunostaining for microglia using the 4C4 antibody in control (top) and Dex-treated retinas (bottom). **(E)** High magnification image of 4C4 staining at 1 dpl control (top) and Dex-treated retinas (bottom). **(F)** The number of TUNEL positive cells at 1 dpl in control (122.27 ± 17.03 cells; n=6) and Dex-treated animals (136.93 ± 8.29 cells; n=6). Scale bar equals 50μm.

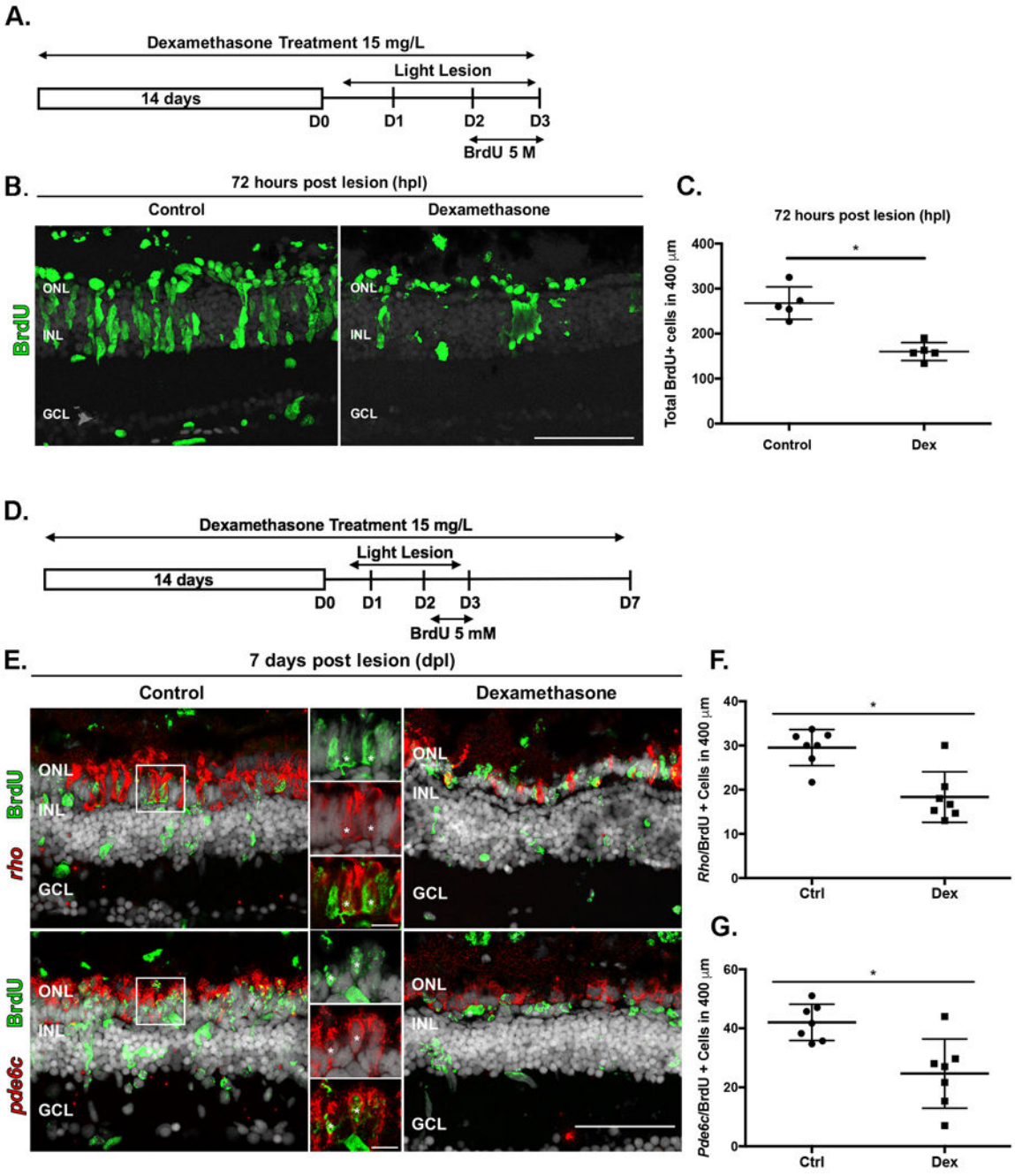

Figure 2: Dexamethasone treatment suppresses proliferation of Muller glia and photoreceptor regeneration.

(A) Experimental paradigm of anti-inflammatory treatment to assay proliferation. **(B)** BrdU immunostained cells (green) in controls (left) and Dex-treated animals (right) at 72 hpl. **(C)** Number of BrdU-labeled cells in controls (268 ± 36.1 cells; n=5) and Dex-treated animals (160.2 ± 20.02 cells; n=5) at 72 hpl; *p=0.0079. **(D)** Experimental paradigm of anti-inflammatory treatment. Regenerated photoreceptors were identified as BrdU-labeled nuclei surrounded by *in situ* hybridization signal for either *rho* (rods) or *pde6c* (cones) at 7 dpl. **(E)** Double labeled, regenerated photoreceptors using *in situ* hybridization for rods (*rho) and*

cones (pde6c; red signal) and BrdU (green). The high magnification insets show the colocalization of the two labels (asterisks). **(F)** Number of regenerated rod photoreceptors in control (29.52 ± 4.1 cells; n=7) and experimental retinas (18.33 ± 5.71 cells; n=7); *p=0.0047. **(G)** Number of regenerated cone photoreceptors in control (42 ± 6.1 cells; n=7) and Dex-treated animals (25 ± 11.72 cells; n=7). *p=0.0012. ONL- outer nuclear layer; INL- inner nuclear layer; GCL- ganglion cell layer. Scale bar equals 50μm.

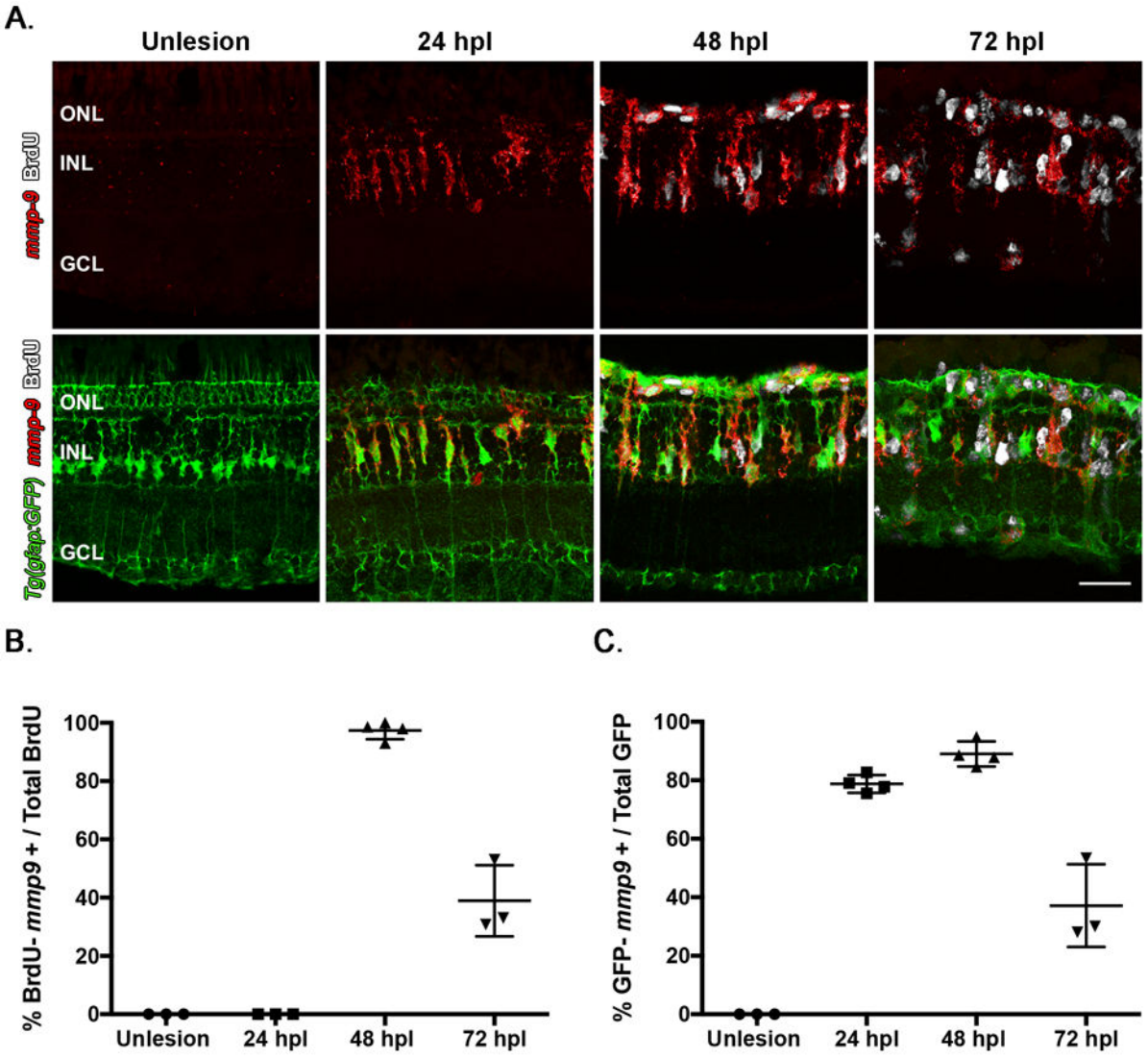

Figure 3: Following a photolytic lesion, Müller glia and Müller glia-derived progenitors express *mmp-9*.

These experiments were performed using the transgenic line *Tg[gfap:EGFP]mi2002*, in which eGFP is expressed in Müller glia. **(A)** Triple labeling using *in situ* hybridization for *mmp-9* (red) and immunostaining for BrdU for dividing cells (white), combined with GFP immunostaining (green). **(B)** Number of BrdU+ cells that express *mmp-9* in unlesioned animals and lesioned animals at 24, 48, and 72 hpl. **(C)** Number of GFP+ Müller glia that also express *mmp-9* expression at 24, 48, and 72 hpl. ONL- outer nuclear layer; INL- inner nuclear layer; GCL- ganglion cell layer. Scale bar equals 25μm.

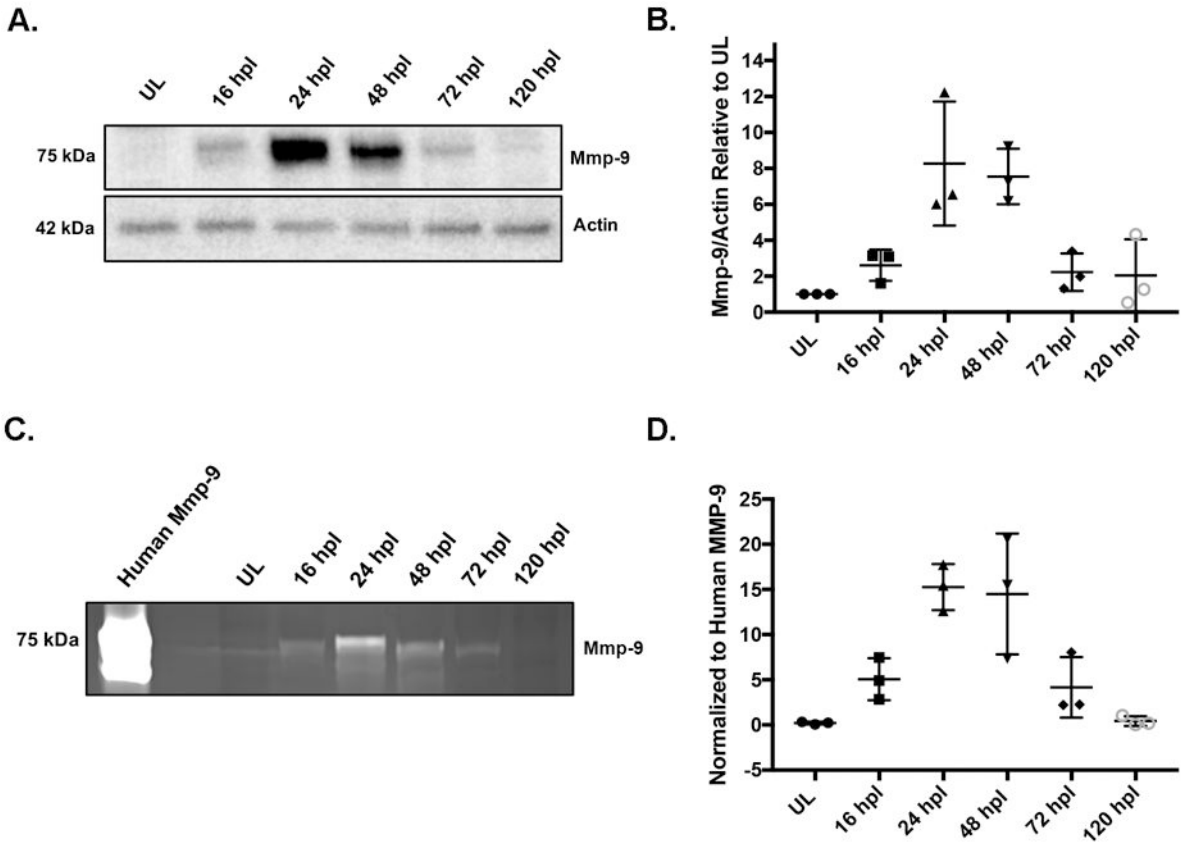

Figure 4: Mmp-9 is expressed and catalytically active following photoreceptor death.

(A) Western blot of retinal proteins from unlesioned retinas (UL) and lesioned retinas at 16 hpl, 24 hpl, 48 hpl, 72 hpl, and 120 hpl, stained with anti-Mmp-9 and anti-actin (loading control) antibodies. **(B)** Densitometry of Mmp-9 protein, plotted relative to unlesioned controls. (ANOVA F-ratio = 8.377, p =.0013) **(C)** Zymogram of Mmp-9 catalytic activity from unlesioned retinas (UL) and lesioned retinas at 16, 24, 48, 72 and 120hpl. Lanes in zymogram correspond to those in the Western blot. Purified human recombinant protein serves as a positive control. **(D)** Densitometry of Mmp-9 catalytic activity, plotted relative to the positive control. (ANOVA F-ratio = 11.870, p =.0003)

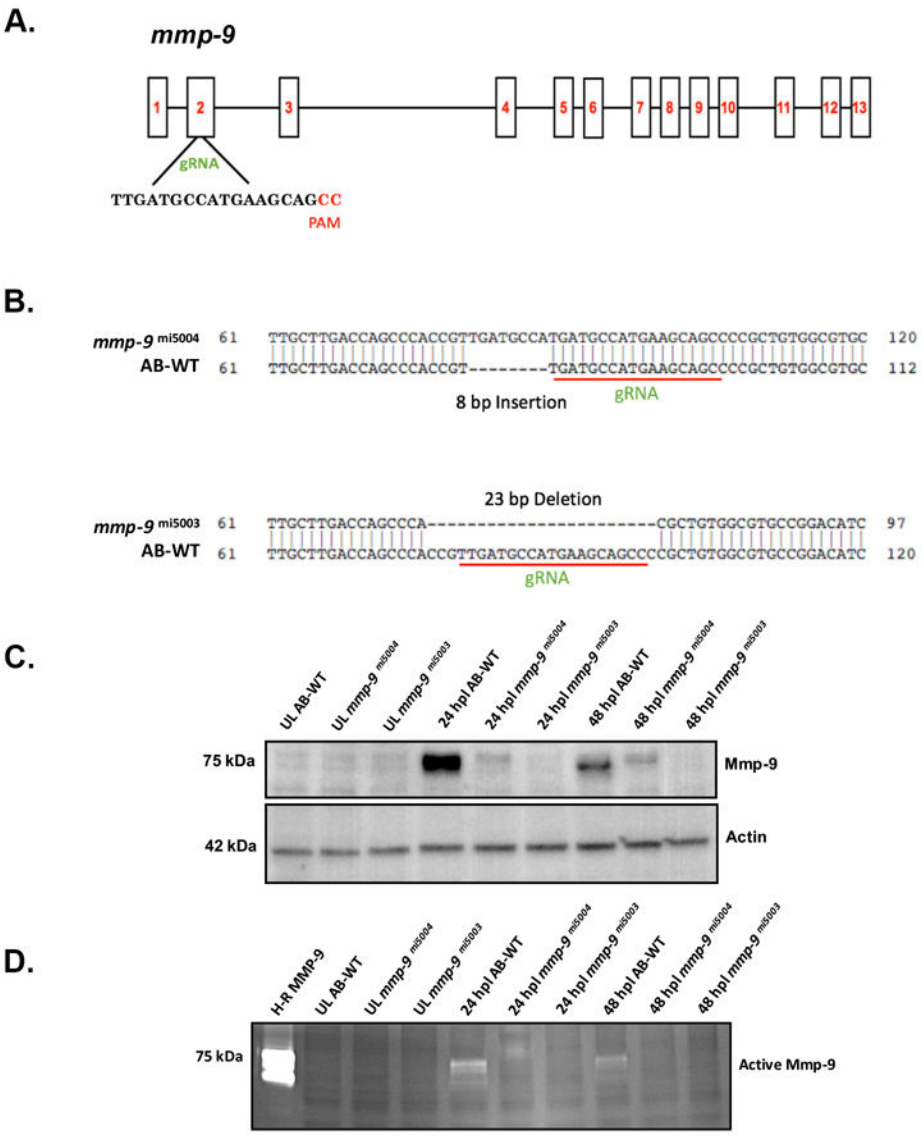

Figure 5: CRISPR mutants lack catalytically-active Mmp-9.

(A) Genomic structure of *mmp-9* and the gRNA target sequence. **(B)** Sequence alignment for two indel mutations - 8 bp insertion (*mmp-9*^{mi5004}) and 23 bp deletion (*mmp-9*^{mi5003}). Red underline indicates the sequence targeted by the 19 bp gRNA. **(C)** Western blot of retinal proteins from unlesioned retinas (UL wild-type; UL *mmp-9*^{mi5004}; UL *mmp-9*^{mi5003}) and lesioned retinas (wild-type; *mmp-9*^{mi5004}; *mmp-9*^{mi5003}) at 16, 24, and 48 hpl stained with anti-Mmp-9 and anti-actin (loading control) antibodies. **(D)** Zymogram of Mmp-9 catalytic activity. Lanes in zymogram correspond to those in the Western blot. Purified human recombinant protein serves as a positive control.

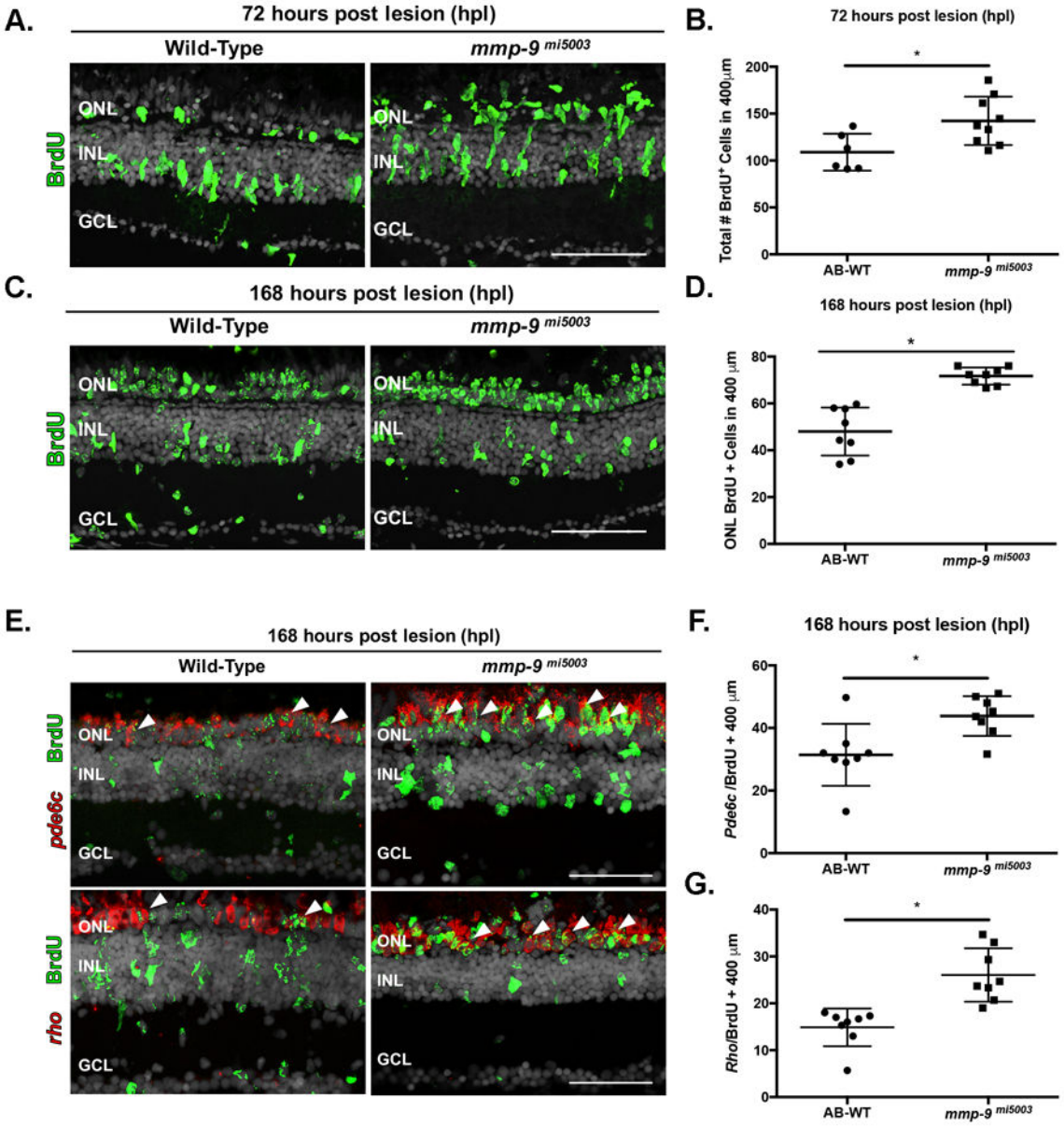

Figure 6: Photolytic lesions in *mmp-9* mutants results in the over production of injury-induced progenitors and regenerated photoreceptors.

(A) BrdU-labeled cells (green) in wild-type and *mmp-9 mi5003*. **(B)** Number of BrdU+ cells from wild-type (109 ± 19.66 cells; n=6) mutant retinas (142.3 ± 25.72 cells; n=9) at 72 hpl. *p = 0.0186. **(C)** BrdU-labeled cells (green) in wild-type and mutant retinas at 168 hpl. **(D)** Number of BrdU+ cells in the ONL of wild-type (48 ± 10.24 cells; n=8) and mutant retinas (71.71 ± 3.7 cells; n=8). *p=0.0001. **(E)** Double labeled, regenerated photoreceptors using *in situ* hybridization for rods (*rho) and cones (pde6c;* red signal) and BrdU (green) at 168hpl. **(F)** Number of regenerated cone photoreceptors in wild-type (31.42 ± 9.88 cell; n=8) and mutant retinas (43.83 ± 10.68 cells; n=8) at 168 hpl. *p=0.0301. **(G)** Number of regenerated rod photoreceptors in wild-type (14.88 ± 4.02 cells; n=8) and mutant retinas (26.04 ± 5.69

cells; n=8) at 168 hpl. *p=0.0005. ONL- outer nuclear layer; INL- inner nuclear layer; GCL- ganglion cell layer. Scale bars equal 50μm.

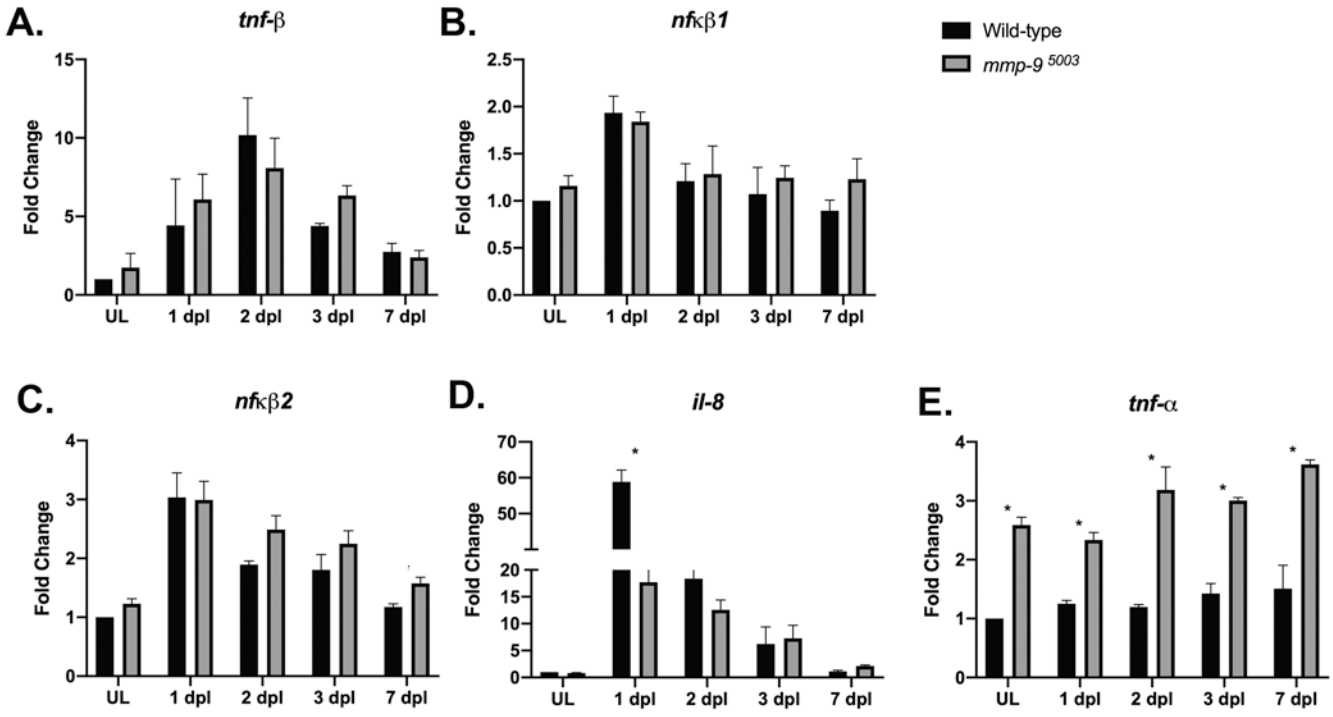

Figure 7: Absence of Mmp-9 results in an altered inflammatory response following photoreceptor death.

Time-course of the expression of inflammatory genes, *tnf-β* **(A**; ANOVA F-ratio =19.2406, p <.0001,), *nfκβ1* **(B**; ANOVA F-ratio= 10.4104, p<.0001), *nfκβ2* **(C**; ANOVA F-ratio= 10.4104, p<.0001), *il-8* **(D**; ANOVA F-ratio= 185.42, p<.0001), and *tnf-α* **(E;** ANOVA F-ratio= 54.53, p<.0001) in Wild-type (black bars) and Mmp-9 mutant (gray bars) retinas following photoreceptor death. Fold changes relative to unlesioned retinas of Wild-type are calculated using DDCt method. ANOVA with post-hoc Tukey, *p<0.0001

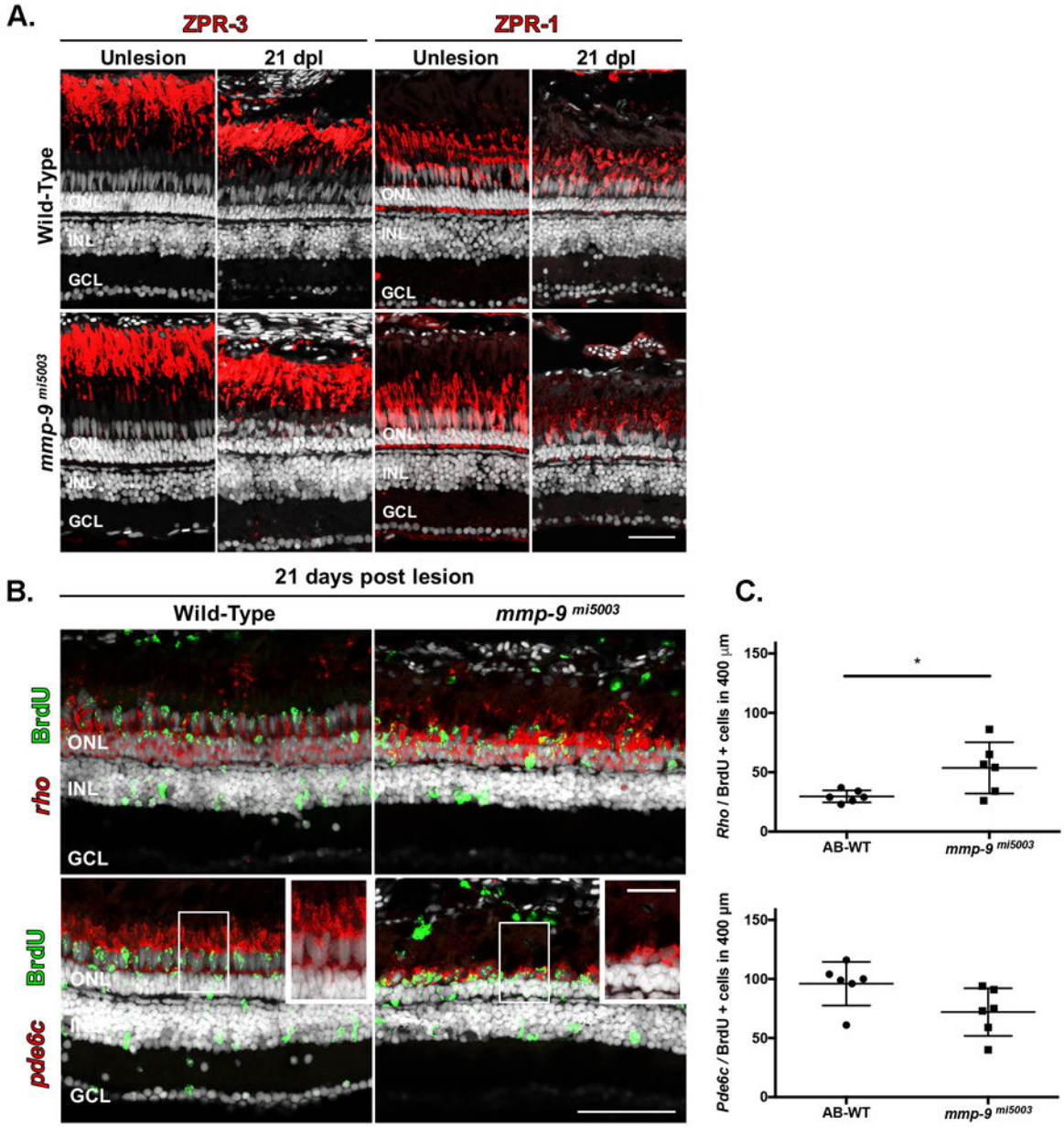

Figure 8. Mmp-9 regulates the survival of regenerated cone photoreceptors.

(A) Immunostaining for red-green double cones with ZPR-1 and rods with ZPR-3. Wild-type are in the top row; mutants are in the bottom row. Unlesioned retinas are left; lesioned retinas at21 dpl are right. **(B)** Double labeled, regenerated photoreceptors at 21dpl using *in situ* hybridization for rods (*rho) and cones (pde6c;* red signal) and BrdU (green). Insets detail the morphology of regenerated photoreceptors in wild-type (left) and mutant retinas (right). **(C)** Number of regenerated cone photoreceptors (bottom) in wild-type (95.81 ± 18.49 cells; n=6) and mutant retinas (71.89 ± 20.37 cells; n=6) at 21 dpl. p=0.059. Number of of regenerated rod photoreceptors (top) in wild-type (29.6 ± 4.94 cells; n=6) and mutant retinas (53.39 ± 21.62 cells; n=6) at 21 dpl. *p=0.0270. ONL- outer nuclear layer; INL- inner nuclear layer; GCL- ganglion cell layer. Scale bar equals 50 μm.

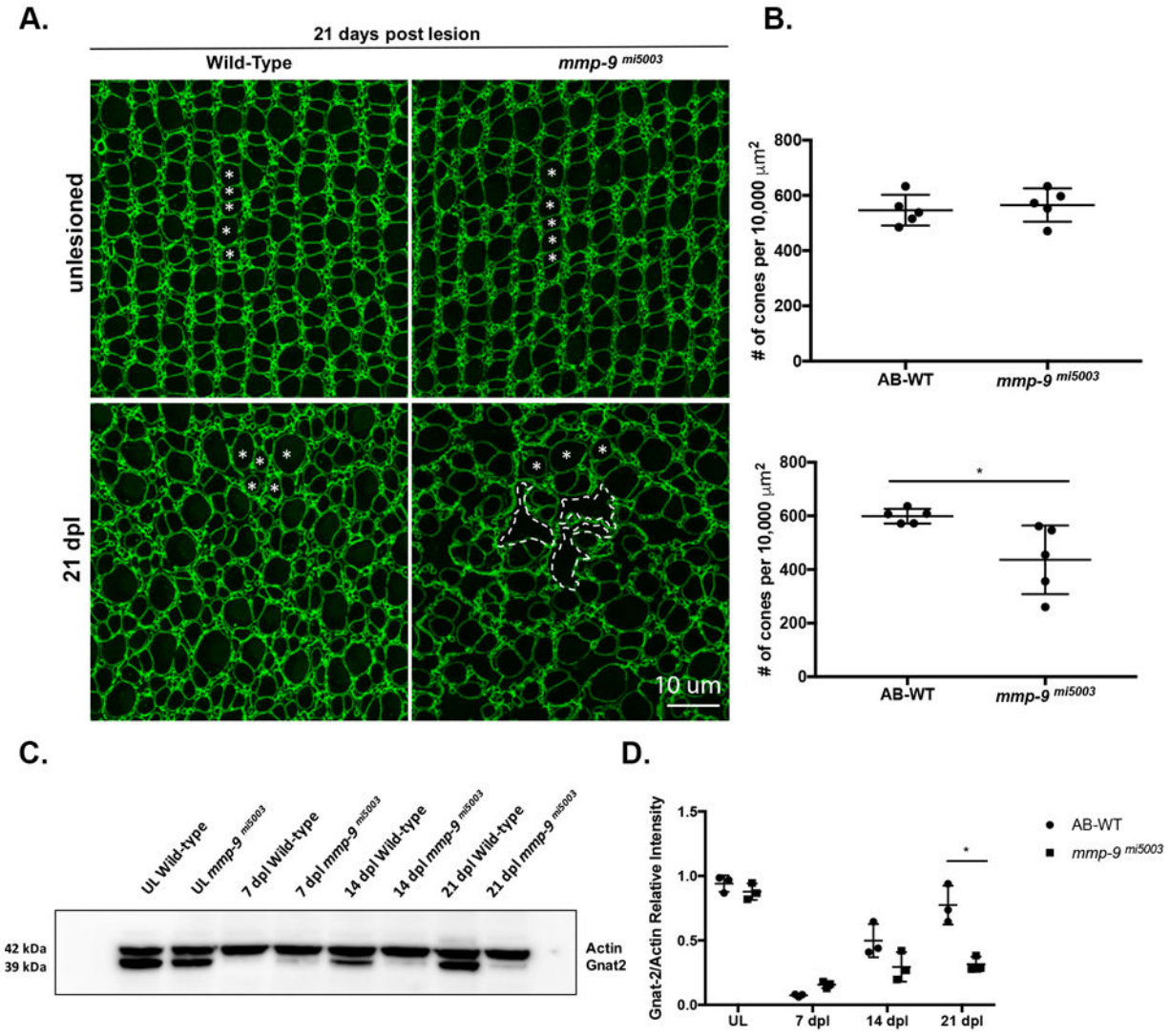

Figure 9. Mmp-9 is required for the survival of regenerated cone photoreceptors.

(A) Wholemounts of wild-type (left) and mutant retinas (right) immunostained for ZO-1. Unlesioned retinas are top; lesioned retinas at 21dpl are bottom. Asterisks indicate profiles of cones. In mutants, gaps due to missing cones are replaced by the irregular apical processes of Müller glia (dashed lines). **(B)** Number of unlesioned cones from wild-type (546.49 ± 55.69; n=5) and *mmp-9 mi5003* (565.33 ± 27.42; n=5) *p=.516; below the number of regenerated cones from wild-type (599.11 ± 27.42 cones; n=5) and mutant retinas (436.09 ± 128.04 cones; n=5) at 21 dpl. *p=0.0238. **(C)** Western blot of retinas stained with antibodies against gnat-2 and actin at 7, 14, and 21 dpl. **(D)** Densitometry of gnat-2 labeling in the Western blot. A significant difference in gnat-2 levels were observed at 21 dpl. *p=.0014. Scale bar equals 10 μm.

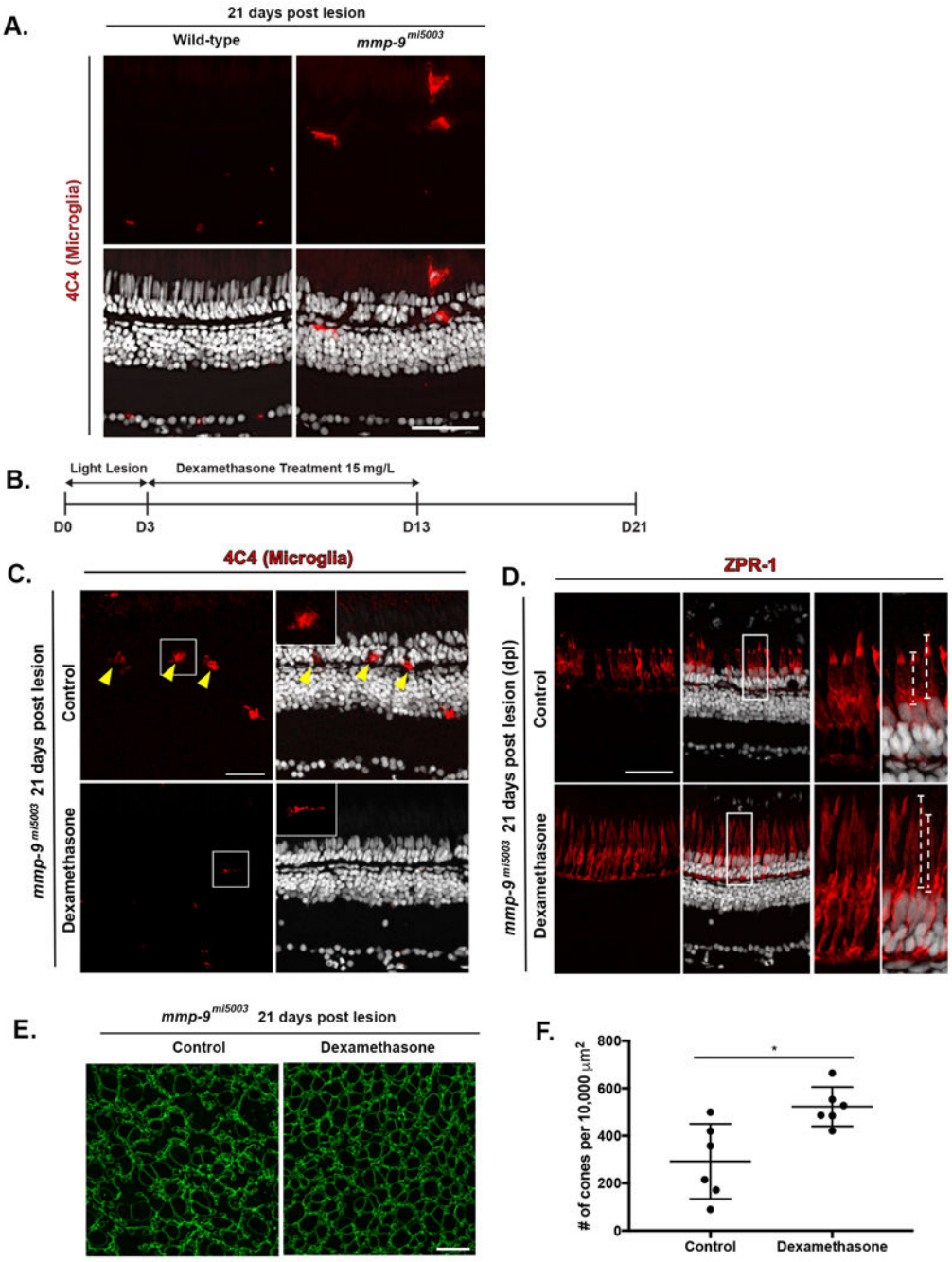

Figure 10: Late anti-inflammatory treatment rescues defects of regenerated cones in mutants at 21 dpl.

(A) Immunostainng for microglia marker, 4C4 in Wild-type (0.1 ± 0.3 cells per 400 µm, n=4) and mutant (4.0 ± 2.2 cells per 400 µm, n=4, p=0.0148) at 21 dpl. (B) Experimental paradigm for the photolytic lesions and Dexamethasone treatment. **(C)** Immunostaining for 4C4 in control (top) and Dex-treated retinas (bottom). Inserts illustrate ameboid (top) and ramified (bottom) microglia. **(D)** Immunostaining with ZPR-1 for red-green double cones in control (top) and Dex mutants (bottom) 21 dpl. Insets illustrate differences in the lengths of the cone photoreceptors (dashed lines; control, 22.1 ± 7.2 µm, n=40 cells; Dex-treated, 29.7

± 4.8 μm, n=69 cells; p<.001) **(E)** Wholemounts of mutant retinas immunostained for ZO-1. Control retina is left; Dex-treated retina is right. **(F)** Number of regenerated cones in control (292.20 ± 158.11 cones; n=6) and Dex-treated retinas (522.79 ± 82.55 cones; n=6) at 21 dpl. Scale bars equal 50 μm in panel A, 40 μm in panels C and D, and 10 μm in E.

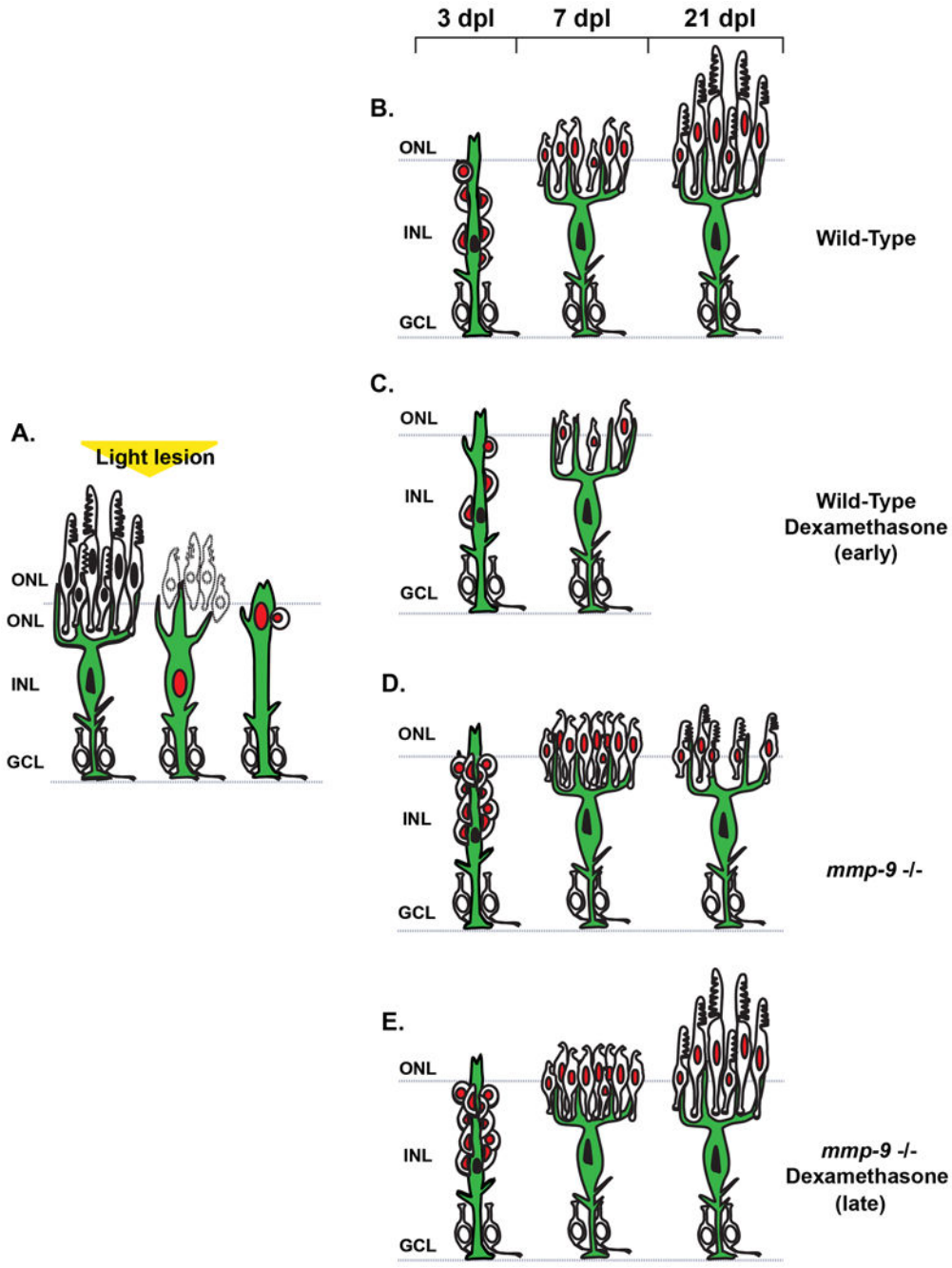

Figure 11. Summary Diagram of cone regeneration

(A) Müller glia respond to photoreceptor death by expressing *mmp-9*, undergoing interkinetic nuclear migration and a single asymmetric cell division that gives rise to a neuronal progenitor. **(B)** In wild-type animals, neuronal progenitors form a neurogenic cluster around the Müller glia (3 dpl), migrate to the ONL, and differentiate into cone photoreceptors (7 dpl) that then mature (21 dpl). **(C)** Anti-inflammatory treatment results in fewer Müller glia-derived progenitors and fewer regenerated photoreceptors. **(D)** In the absence of Mmp-9, there is overproduction of Müller glia-derived progenitors and regenerating photoreceptors. However, at 21 dpl, survival of cone photoreceptors is

compromised. **(E)** In the absence of Mmp-9, anti-inflammatory treatment rescues the defects of cone photoreceptors. ONL- outer nuclear layer; INL- inner nuclear layer; GCL- ganglion cell layer.

Table 1:

Primer Sequences

Name	Sequence
gpia	F) 5'- TCCAAGGAAACAAGCCAAGC-3' R) 5'- TTCCACATCACACCCTGCAC-3'
mmp-9	F) 5'- TGATGTGCTTGGACCACGTAA-3' R) 5'- ACAGGAGCACCTTGCCTTTTC-3'
tnf-α	F) 5'- GCGCTTTTCTGAATCCTACG-3' R) 5'- TGCCCAGTCTGTCTCCTTCT-3'
tnf-β	F) 5'- CCTCAGACCACGGAAAAGT-3' R) 5'- GCCCTGTTGGAATGCCTGAT-3'
il-6	F) 5'- TCTTTCCCTCTTTTCCTCCTG -3' R) 5'- TCAACTTCTCCAGCGTGATG -3'
il-8	F) 5'- GTCGCTGCATTGAAACAGAA -3' R) 5'- AGGGGTCCAGACAGATCTCC-3'
nfκb1	F) 5'- ACCAGACTGTGAGCGTGAAG -3' R) 5'- CGCAAGTCCTACCCACAAGT -3'
nfκb2	F) 5'- CATATGTCCCACACAATCAAGAC-3' R) 5'- AGCCACCATAATGATCTGGAA -3'
stat3	F) 5'- GAGGAGGCGTTTGGCAAA -3' R) 5'- TGTGTCAGGGAACTCAGTGTCTG -3'
gfap	F) 5'- AGGCTCATGTGAAGAGGAGCATAG -3' R) 5'- CCTCATTATGGCAGATCCTTCCTC -3'

Table 2:

Antibody List

Primary Antibodies	Company	Dilution
Mouse monoclonal anti-GFP	Milipore MAB3580	1:200
Mouse monoclonal anti-actin	Calbiochem	1:1000
Mouse Monoclonal anti-Zn5	ZIRC; zfin.org/ZDB-ATB-081002-19	1:200
Mouse Monoclonal anti-Zpr1 (anti-Arrestin-3)	ZIRC; zfin.org/ZDB-ATB-081002-43	1:200
Mouse Monoclonal anti-Zpr-3	ZIRC; zfin.org/ZDB-ATB-081002-45	1:200
Mouse anti-HPC1	ZIRC; zfin.org/ZDB-ATB130225-1	1:200
Mouse anti-Zrf1	ZIRC; zfin.org/ZDB-ATB-081002-46	1:1000
Mouse Monoclonal ZO-1A-12	Innovative Research Cat# 33-9100, RRID:AB_87181	1:200
Mouse anti-BrdU	BD Biosciences Ca# 347580	1:100
Rat anti-BrdU	Abcam Cat# ab6326, RRID:AB_305426	1:200
Polyclonal anti-GNAT2	MBL Ca# PM075	1:1000
Mouse Monoclonal anti-1D1 (ZF Rhodoposin)	Hyatt et al., 1996 Gift from Dr. Jim Fadool (FSU)	1:1000
Mouse Monoclonal anti-4C4 (zebrafish microglia)	Raymond et al., 2006 Hitchcock Lab	1:200
Polyclonal anti-mCherry antibody	Abcam ab167453	1:200
Secondary Antibodies		
Alexa Fluor goat anti-mouse 488, 555, or 647	Invitrogen	1:500
Alexa Fluor goat anti-rabbit 488, 555, or 647	Invitrogen	1:500
Alexa Fluor goat anti-rat 488, 555, or 647	Invitrogen	1:500